ECMWF Newsletter

Number 141 – Autumn 2014

European Centre for Medium-Range Weather Forecasts
Europäisches Zentrum für mittelfristige Wettervorhersage
Centre européen pour les prévisions météorologiques à moyen terme

www.ecmwf.int/en/about/news-centre/media-resources

CONTENTS

PUBLICATION POLICY

The *ECMWF Newsletter* is published quarterly. Its purpose is to make users of ECMWF products, collaborators with ECMWF and the wider meteorological community aware of new developments at ECMWF and the use that can be made of ECMWF products. Most articles are prepared by staff at ECMWF, but articles are also welcome from people working elsewhere, especially those from Member States and Co-operating States. The *ECMWF Newsletter* is not peer-reviewed.

Editor: Bob Riddaway

Typesetting and Graphics: Anabel Bowen with the assistance of Simon Witter.

Any queries about the content or distribution of the *ECMWF Newsletter* should be sent to Bob.Riddaway@ecmwf.int
Guidance about submitting an article is available at www.ecmwf.int/en/about/news-centre/media-resources

CONTACTING ECMWF

Shinfield Park, Reading, Berkshire RG2 9AX, UK		
Fax:		+44 118 986 9450
Telephone:	National	0118 949 9000
	International	+44 118 949 9000
ECMWF website		www.ecmwf.int

Copernicus and ECMWF

The 11th November 2014 was a very significant day for ECMWF as we signed an agreement with the European Commission for ECMWF to manage the Copernicus Atmosphere Monitoring Service and the Climate Change Service. The two services represent an investment by the EU of €291 million over seven years and they will involve scientific and technical contributions from across Europe. The information provided by the two services will help businesses, policy-makers and citizens cope with the impacts of climate change and poor air quality, for example.

The Atmosphere Monitoring Service will combine state-of-the-art numerical models of the atmosphere, such as those used for the daily weather forecasts, with satellite and in-situ observations to provide daily forecasts of the composition of the air around the globe with a particular focus on Europe. It will deliver up-to-date information in a number of areas of high societal relevance, including air quality, climate forcing, ozone layer and UV radiation, solar radiation and solar energy resources, and emissions of pollutants and greenhouse gases.

The Climate Change Service will build on and complement capabilities existing at national level and will become a major contribution from the European Union to the WMO's Global Framework for Climate Services. It will provide comprehensive climate and climate change information covering the atmosphere, land, ocean, sea-ice and carbon, for timescales spanning decades to centuries. It will use past, current and future Earth observations (from in-situ and satellite observing systems), state-of-the-art modelling, supercomputing and networking capabilities. This will produce a consistent, comprehensive and credible description of the past, current and future climate.

This is an important development with many benefits for different organisations and people in Europe (and elsewhere). But the reader will perhaps indulge me as I now reflect more narrowly the benefits for ECMWF. From a scientific viewpoint it enables us to accelerate the move towards an Earth-system science approach to modelling, analysis and prediction of the weather and other related aspects of the natural environment. It establishes ECMWF as an entity entrusted by the European Union to manage some key European environmental information services. It also signals that weather and climate science and technology are intimately connected and that both will benefit from an even closer union – as indeed will the eventual formulation of environmental policies.

Of course from a funding viewpoint, Copernicus services at ECMWF secure stability for seven years in the areas for which ECMWF is responsible. In addition, given the collaborative approach the Centre will pursue, most of this funding will be for other service providers across Europe.

Like all publicly funded organisations, ECMWF has to provide value for the money invested in it. With the addition of Copernicus services to the Centre's activities, the infrastructure at the Centre – both human and physical – will be used even more extensively for the benefit of European citizens, improving our cost–effectiveness. This should also help us build an even stronger case for increased investment in supercomputing at ECMWF. Critically, these benefits will also lead to ECMWF becoming even more attractive to the best scientific and technical minds in Europe as a place to work and as a place to interact with.

Alan Thorpe

Copernicus Climate Change and Atmosphere Monitoring Services

BOB RIDDAWAY

An agreement was signed in Brussels 11 November 2014 between the European Commission and ECMWF. This agreement means that ECMWF will be managing the Copernicus Climate Change and Atmosphere Monitoring Services.

The European Union's flagship Copernicus programme ensures operational monitoring of the atmosphere, oceans, and continental surfaces, and will provide reliable, validated information services for a range of environmental and security applications. It comprises six services that provide reliable and consistent environmental information: Land Monitoring, Marine Monitoring, Atmosphere Monitoring, Emergency Management, Security, and Climate Change.

Examples of Copernicus products

Climate Change Service

- Consistent estimates of multiple Essential Climate Variables.
- Global and regional reanalyses.
- Products based on observations alone.
- Near-real-time climate monitoring.
- Multi-model seasonal forecasts.
- Climate projections at global and regional scales.

Atmosphere Monitoring Service

- Daily production of near-real-time analyses and forecasts of global atmospheric composition and European air quality.
- Reanalyses of atmospheric composition and European air quality.
- Solar and UV radiation products.
- Surface flux inversions of greenhouse gases.
- Climate forcings from aerosols and other agents.

Signing of the agreement for two Copernicus services managed by ECMWF. The agreement was signed by Alan Thorpe, Director-General of ECMWF, and Daniel Calleja, Director General, DG Enterprise and Industry, European Commission, on 11 November 2014 in Brussels.

The Copernicus Climate Change and the Atmosphere Monitoring Services represent an investment by the EU of €291 million over seven years and will draw together contributions from across Europe. The main users of these Copernicus services will be policy-makers and public authorities who need the information to develop environmental legislation and policies or to take critical decisions in the event of an emergency, such as a natural disaster or a humanitarian crisis. In addition, many value-added services will be tailored to specific public or commercial needs, resulting in new business opportunities.

ECMWF's Director-General Alan Thorpe said:

"The Copernicus programme is a milestone for Earth observations and its many scientific and operational applications. The two services that ECMWF is managing are vital to provide to European policy-makers, businesses and society at large the highest quality environmental information. ECMWF will build upon its expertise in these fields and its extensive scientific and technical partnerships across Europe and beyond to lead this ambitious and extremely timely initiative. There is a critical need for science-based and user-driven services to be made available to policy-makers and citizens alike, and the EU's investment in the Copernicus Services will deliver just that."

Speaking at the joint session where agreements for three Copernicus Services were being signed – Mercator, the French centre for ocean analysis and forecasting taking on Marine Monitoring, and ECMWF for Climate Change and Atmosphere Monitoring – Daniel Calleja, Director General, DG Enterprise and Industry, European Commission said:

"The signature of these delegation agreements represents another major milestone for the Copernicus programme towards full operational status. The European Centre for Medium-Range Weather Forecasts and Mercator Océan are the best possible partners for the Commission to implement the Copernicus services for monitoring the Atmosphere, Climate Change and the Marine Environment. Together we will develop services which will both support policy-making and stimulate the economy to the benefit of European citizens."

More information about the Copernicus Climate Change and Atmosphere Monitoring Services is available at:

http://www.ecmwf.int/en/about/what-we-do/copernicus/copernicus-climate-change-service

http://www.ecmwf.int/en/about/what-we-do/copernicus/copernicus-atmosphere-monitoring-service

Recent cases of severe convective storms in Europe

IVAN TSONEVSKY, LINUS MAGNUSSON, TIM HEWSON

Summer 2014 was characterised by a widespread negative anomaly of 500 hPa geopotential height centred over Western Europe (first figure). The whole season has been very active in terms of severe convection. Three cases of major convective storms over Europe are presented. The study of these cases, along with user feedback, indicates that there would be benefit in developing severe weather products focussed on forecasting deep convection.

9 June

On 9 June, following a period of hot weather, a severe convective outbreak affected Western Europe. In Germany six people were killed, mainly by falling trees. Deep moist convection developed along the western fringe of a hot air mass.

Strong wind gusts were reported from many sites in France, Belgium, the Netherlands and Germany, widely exceeding 20 m/s, in a few cases exceeding 25 m/s and with a peak of 42 m/s at Düsseldorf airport (second figure). The ECMWF ensemble forecast (ENS) failed to give a signal of strong winds: probabilities of wind gusts exceeding the 95th percentile of the model climate (M-climate) are fairly small. As a reference, the values of the 95th percentile of the M-climate are in the range 14 to 17 m/s. However, looking at the Convective Available Potential Energy (CAPE) as a predictor of the convective instability of the atmosphere, the ENS shows a very high chance of CAPE exceeding the 95th percentile of the M-climate.

Instability is one of the three key ingredients of severe convection and the high values in this case are a good indicator of the risk of severe thunderstorms and thus of possible strong convective wind gusts. Heavy rain associated with convection was much better captured by both the ECMWF high-resolution forecast (HRES) and ENS. This case illustrates the need to complement the ECMWF severe weather products (e.g. the Extreme Forecast Index, EFI), with a parameter that is suitable for forecasting severe convection.

19 June

Severe thunderstorms developed over south-eastern Europe on 19 June. More than 100 mm of rain fell in north-eastern Bulgaria in just a few hours causing a number of fatalities, most of them during a deluge in a residential area of the coastal city of Varna. Convective storms developed underneath an upper-level trough with active surface cyclogenesis simultaneously occurring over the western part of the Black Sea.

The convective nature of the precipitation makes forecasts of its location and intensity particularly difficult. The uncertainty in the forecast remained large even in the short range. In such situations, high-resolution limited-area ensembles can help in assessing the uncertainty by showing, for example, the probability of precipitation greater than a particular threshold (third figure). These ensembles form part of the TIGGE-LAM project and are available through the ECMWF archive system – they are a valuable source of data for case studies and for forecast evaluation.

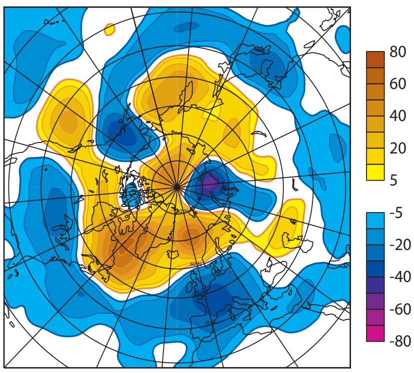

1: Anomalies of 500-hPa geopotential height for June to August 2014 (in m). This shows that a widespread negative anomaly of 500 hPa geopotential height was centred over Western Europe during the summer of 2014. The anomalies are with respect to ERA-Interim. Note that a simple normalisation has been applied to ensure a zero mean anomaly over the domain; without this positive anomalies would look much more prominent, due to a general increase in 500 hPa height over recent decades.

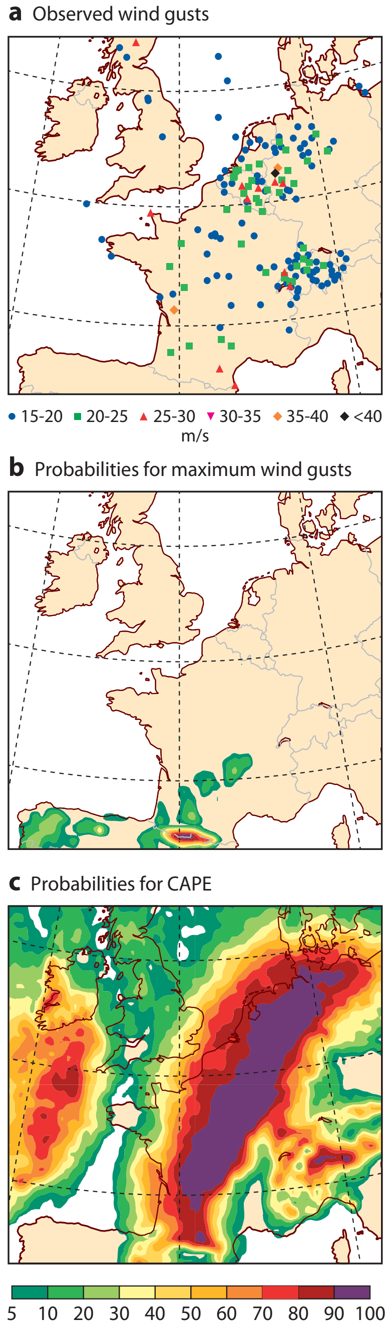

2: Observed wind gusts and ENS probabilities for 9 June 2014. (a) Observed maximum wind gusts (in m/s) on 9 June 2014. (b) Probability of maximum wind gusts in the 24- to 48-hour forecast exceeding the 95th percentile of the M-climate – this did not give a signal that strong winds might occur even in the very short range. (c) Probability of CAPE in the 72- to 96-hour forecast exceeding the 95th percentile of the M-climate – this gave a strong signal that high values of CAPE might occur over a large area well in advance.

TIGGE-LAM is a high-resolution, limited-area model extension of the TIGGE initiative (THORPEX Interactive Grand Global Ensemble), which involves the regular archiving of weather forecasts from ensembles.

31 August

Quasi-stationary convective storms caused significant flooding in Copenhagen and Malmo on 31 August. Roads were closed and buildings flooded. Convection occurred in the vicinity of an occluded front.

High-density observations around Copenhagen, provided on the Danish Meteorological Institute (DMI) website, show some massive precipitation totals in excess of 100 mm, but with large spatial variations across the city. Over 100 mm was also recorded locally in Malmo. These variations occurred within an HRES grid box (~16 km) and as such cannot be captured directly. For the same reason, one should not expect the probability of heavy rain as measured at individual points to be given directly by ensembles either, particularly those run at lower resolution.

As shown in the fourth figure, high-resolution ensembles (COSMO-LEPS ~10 km, DMI-HIRLAM ~5.5 km, COSMO-DE-EPS ~2.8 km) show more detail and generally higher probabilities compared to the ECMWF ENS (~32 km). The ENS can, however, be compared to its own model climatology, via the non-dimensional metrics that ECMWF uses for this purpose, namely the EFI and the complementary Shift of Tails (SOT) (for more details see *ECMWF Newsletter No. 107*). The EFI and SOT for this event are plotted on the fifth figure. Evidently the ENS did provide signals in advance that an extreme precipitation event was possible.

Current status and future developments

The active convective season in Europe this summer, and indeed user feedback, have both highlighted a need to put more effort into developing severe weather products focused on forecasting deep convection. With these we will be able to take full advantage of recent improvements in the Integrated Forecasting System (IFS) and the resolution upgrade planned for next year.

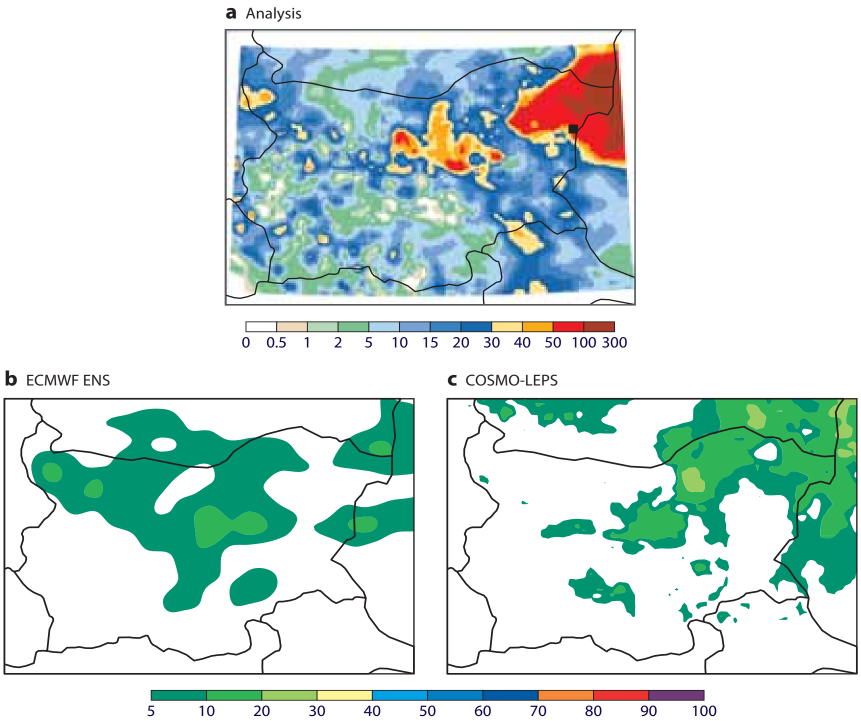

3: Analysis and probabilities of precipitation exceeding 50 mm/24 hours for 19 June 2014. (a) Analysis of precipitation from 06 UTC on 19 June to 06 UTC on 20 June 2014 obtained by ALADIN LAM Bulgaria in combination with a high-density rain-gauge network (courtesy of the National Institute of Meteorology and Hydrology, Bulgaria). (b), (c) Forecasts of the probability of precipitation greater than 50 mm/24 hour from ECMWF ENS and COSMO-LEPS respectively. The high-resolution ensemble forecast from COSMO-LEPS provided more details and could help assess the uncertainty in the short-range forecasts. Both forecasts show probabilities higher than the climatological probabilities. All the forecasts are for 54- to 78-hour lead times. The grid spacing of ECMWF ENS is about 32 km and for COSMO-LEPS it is about 10 km. The black square on the precipitation analysis map denotes the coastal city of Varna that suffered floods and fatalities.

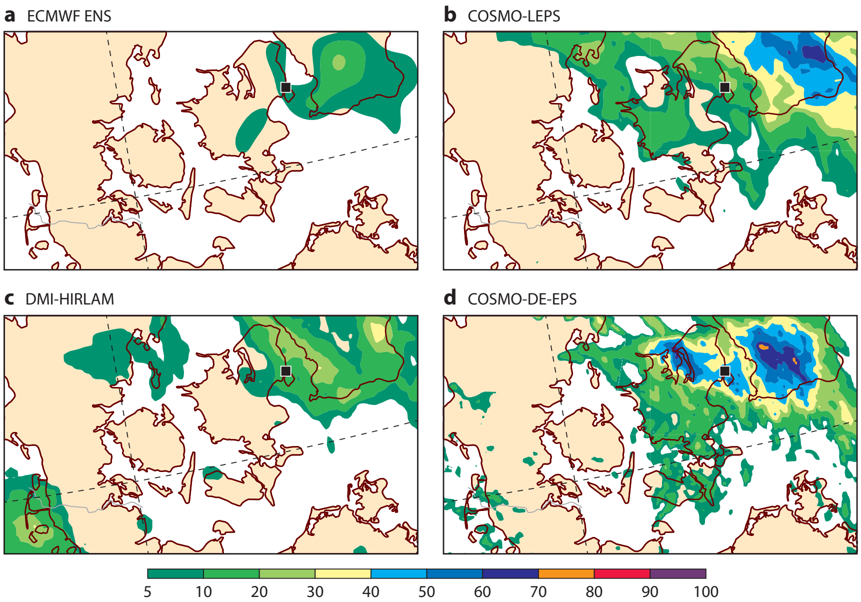

4: Probability of precipitation above 20 mm/12 hours for 31 August 2014. Forecasts are valid from 00 to 12 UTC on 31 August 2014 from ensemble runs at 12 UTC on 30 August from (a) ECMWF ENS (~32 km grid spacing), (b) COSMO-LEPS (~10 km), (c) DMI-HIRLAM (~5.5 km), and (d) COSMO-DE-EPS (~2.8 km). The high-resolution ensemble forecasts show details and generally higher probabilities compared to the ECMWF ENS. The black square is Copenhagen.

The TIGGE-LAM archive helps us evaluate the performance of the IFS in severe weather by allowing us to compare its performance directly with that of limited-area ensembles.

The above discussion has focussed on lead times up to about three days, and has shown that the IFS can provide some very useful pointers for forecasters. For the three cases we have also assessed IFS products, such as the EFI, for longer lead times. These products also contain some signals pointing to the possibility of severe weather, and for the first case a strong CAPE signal was in the right place up to 5 or 6 days in advance. But for the other cases the signals were quite weak and would not have provided much assistance in pinpointing the most vulnerable areas. For other types of extreme weather, EFI signals tend to be more useful than this at longer leads. We believe that these differences in performance simply reflect the fact that certain types of weather extreme are more difficult to predict than others.

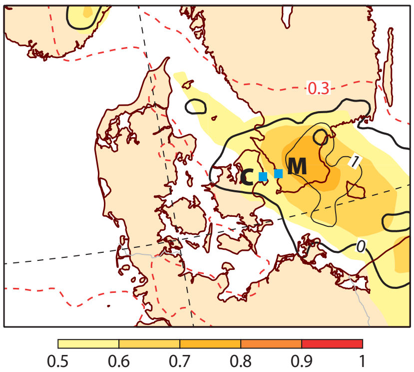

5: EFI and SOT for total precipitation for 31 August 2014. The 48- to 72-hour forecast from 00 UTC on 29 August shows that ENS provided a signal of extreme precipitation. The EFI shadings highlight the areas that are most vulnerable to a heavy precipitation event, whilst the SOT contours indicate that in some regions at least 10% of ensemble members show an outcome that is particularly extreme. Blue squares with the letters are Copenhagen (C) and Malmö (M). Note that the innermost contour in southern Sweden indicates an SOT value of 2.

For those with suitable ECMWF web access credentials, information about more severe weather cases around the world and particularly across Europe can be found via: https://software.ecmwf.int/wiki/display/FCST/Forecast+User+Home.

On these web pages users can also find out about some known issues with and limitations of the ECMWF forecasting system. There is also an opportunity for users to provide feedback and share additional information about the performance of the IFS, and any case study material, such as high density observations, that they have.

Licensing ECMWF products

CRISTIAN CODOREAN, CHRISTOPHE SEYNAEVE, FABIO VENUTI

ECMWF real-time forecast products are more popular than ever among commercial companies. The latest projections show that by the end of 2014 ECMWF may record more than 130 standard commercial licences, with an increase of about 12% compared to last year. The number of maximum-charge customers (32), which constantly increased up to 2013, will remain substantially unchanged in 2014. This may be a sign that the meteorological industry is undergoing changes that imply the consolidation of larger companies, as also noted by a study commissioned by EUMETNET. Compared to 2011, these figures represent a 59% increase in the number of standard commercial licences and a 65% increase in the number of maximum-charge licences. In terms of the revenue in euros from product sales, the estimated increase compared to last year is around 12%.

ECMWF products are licensed by Member and Co-operating States and by ECMWF itself. The biggest licensors are the UK Met Office, ECMWF and the Norwegian Meteorological Institute. Tom Mcilwaine, Data Wholesaling Manager at the UK Met Office, states that "the Met Office has seen annual growth in the number of data licences agreed. The growth has largely been attributed to the increasing awareness of ECMWF's model data across the globe and the high standard of service delivered by ECMWF. We expect licence revenue to grow as businesses increasingly understand the benefits of incorporating ECMWF data into their products and services".

ECMWF provides support to the catalogue contact points, who manage the licensing activity of Member and Co-operating States, co-ordinates their reporting and consolidates the related financial information. To improve and simplify the flow of information, ECMWF has developed a web application that allows catalogue contact points to easily add and renew contract reports, calculate the shares due to ECMWF, and keep track of invoice payments and contract expiration. The application is integrated with ECMWF's accounting system and provides an overall view of ECMWF product sales.

The application, written in Python, uses Django, JavaScript, and jQuery technologies and is integrated in the newly deployed framework for delivering ECMWF's 'Web On Demand' services.

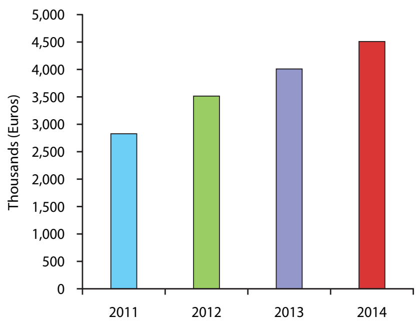

Evolution of ECMWF's revenue from product sales. It is estimated that during 2014 there will be a 59% increase in revenue, excluding handling charges, with respect to revenue in 2011.

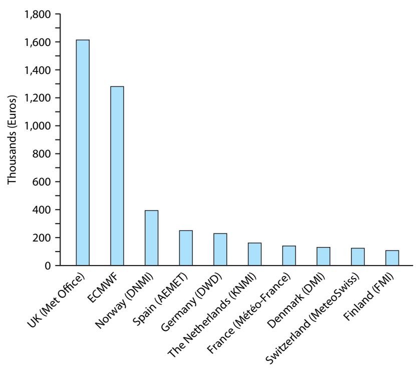

Top ten licensors of ECMWF products in 2014. Three licensors generate 73% of the data licensing revenue: UK Met Office, ECMWF and the Norwegian Meteorological Institute.

Closing the GRIB/NetCDF gap

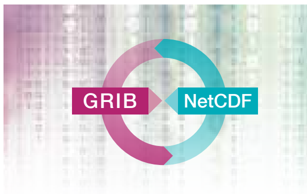

MANUEL FUENTES,
BAUDOUIN RAOULT,
KEVIN MARSH

Data presented to users in GRIB (GRIdded Binary) is often not fully utilised by groups who work primarily with NetCDF (Network Common Data Form), and vice versa. This is a vital issue and one which can be a major barrier to maximising data use and reuse by different user communities.

At ECMWF, the Meteorological Archival and Retrieval System (MARS) has around 50 PB of data stored, much of it in GRIB format. However, there is a growing need to make more of this data available in NetCDF format to encourage its usage within new user communities, though there are problems in doing this.

- Conversion of data (and metadata) between the two forms is often non-trivial and can be fraught with difficulties.
- The quantity and quality of the metadata provided with the data can be highly variable, and restrict greater interoperability.

Also, while GRIB will remain the main data format in MARS, new datasets are being generated which are already in NetCDF (e.g. NEMO ocean model outputs). One such dataset is the CERA-20C coupled analysis over the 20th century which will be produced at ECMWF. Here, the atmospheric and wave model fields are in GRIB, while the ocean model fields are in NetCDF files output directly from NEMO. These data will also require archiving in MARS, and a clear 'roadmap' for the way forward is required to enable this to happen.

In order to bring the two communities together, ECMWF organised an international workshop on 'Closing the GRIB/NetCDF Gap', which was held at ECMWF on 24 and 25 September 2014. The participants were experts and stakeholders from the various communities, and the aim was to discuss how to close the 'gap' and formulate a common 'roadmap' for the way forward. The issues discussed included how standards-based mappings between GRIB and the Climate and Forecasts (CF) Metadata conventions can be established and maintained, and how the governance models of the various communities can work together. Note that the views expressed were personal and did not necessarily reflect those of their organisations.

At the start of the first day, a welcoming address was given by Florence Rabier, Director of Forecasts at ECMWF. This outlined the goals of the workshop, and was followed by a presentation from Baudouin Raoult of ECMWF which 'set the scene' for the technical issues to be addressed. There were then 14 invited presentations from various domain experts which mainly dealt with aspects of governance and data standards, and which promoted a lively debate. The presentations were also streamed live via WebEx on both days to expert colleagues at UNIDATA in the United States.

The meeting was then split into two groups to begin discussions on the chosen themes for the Workshop – 'Mappings' and 'Governance', which were chaired by John Caron (UNIDATA) and Simon Elliott (EUMETSAT). These broad themes were selected as it was felt that they reflected the 'Present' and 'Future' of GRIB/NetCDF interoperability. A plenary session was held at the end of the first day to present the initial findings from the working groups and discuss the issues raised.

The second day followed a similar structure to the first, with eight presentations describing issues such as 'real-world' implementations in archives, and software tools which are useful when converting data between GRIB and NetCDF. The remainder of the day was taken up by further working group discussions. The 'Mappings' group decided that there were several important areas of interest, and so decided to create subgroups concerned with the issues of 'Parameters/Standard_Names/Units and Statistical Processes/Cell Methods', 'Tools', and 'Mappings'. This allowed them to focus in on the given topic and make rapid progress. A final plenary session was held at the end of the day to discuss the findings of the four working groups. The workshop closed with Manuel Fuentes of ECMWF giving a summary of the meeting.

The presentations and proceedings are available at: http://www.ecmwf.int/en/workshop-closing-grib/netcdf-gap. Also further information about GRIB and NetCDF can be found at:

- GRIB Introduction: http://www.wmo.int/pages/prog/www/WMOCodes/Guides/GRIB/Introduction_GRIB1-GRIB2.pdf
- CF-NetCDF: http://cfconventions.org/
- NetCDF: http://www.unidata.ucar.edu/software/netcdf/

The outcome of the workshop will allow ECMWF to ensure that NetCDF data is fully supported within MARS, and that the data is used to its maximum potential.

A 'roadmap' for the way forward

A 'roadmap' for the way forward is outlined below. This arose as a result of the workshop discussions and findings of the working groups.

- Set up a dedicated wiki area and mailing list – *This 'first step' could possibly be done under IS-ENES, and publicised by existing means.*
- Select a core set of features initially – *Such as the master tables of GRIB edition 2 and CF-NetCDF.*
- Extract mappings information from existing tools – *Utilise existing knowledge as another 'first step'.*
- Store mappings information in 'METARELATE' – *Use an existing system to store the information.*
- Store additional information on tools and mappings in the wiki area – *So that knowledge can be shared amongst the community.*
- Create sample files as examples of 'best practice' and guidelines – *To encourage a more consistent approach amongst data producers and providers.*

Participants at the "Closing the GRIB-NetCDF Gap" Workshop. Over 30 experts attended the two-day workshop. These included experts in NetCDF, the Climate and Forecasts (CF) Metadata conventions, and WMO experts in Table Driven Code Forms (GRIB) . In addition, numerous ECMWF staff attended the workshop presentation sessions and took part in the Breakout Group discussions.

Peter Janssen awarded the EGU Fridtjof Nansen Medal for 2015

ERLAND KÄLLÉN,
JEAN BIDLOT

Peter Janssen has been awarded the Fridtjof Nansen Medal for 2015 by the European Geosciences Union. This medal has been established in recognition of the scientific achievements of Fridtjof Nansen and is awarded for distinguished research in oceanography.

Peter is a world leader on the theory and modelling of ocean waves. He was a major contributor to the third-generation wave model (WAM). Modern wave forecasting is based on concepts first put forward during the development of WAM. It was under his leadership that a global version of WAM was first implemented operationally at ECMWF.

Most importantly, Peter's work has highlighted the necessity of truly coupling the surface ocean waves with the atmosphere. Peter's research has shown the role of surface waves in the transfer of momentum and energy across the air-sea interface. Also he developed a new theory of how waves can modify the air flow and he included this effect for the first time in WAM. The theory and approach he proposed have since been widely adopted. Ultimately, Peter knew that this feedback of the waves on the atmospheric circulation had to be included in the atmospheric model. Undeterred by the challenge of coupling two separate operational models, Peter ensured that ECMWF implemented the two-way coupled system in the late nineties. This system has been the backbone of world-class ocean wave forecasts and analyses that are provided by ECMWF.

Recently, Peter developed and implemented an operational freak wave warning system based on his pioneering theoretical work. Freaks waves are abnormally large waves that can wreak havoc over the oceans. Incidentally, his theory for freak waves has also found application in non-linear optics because the common physical process is the formation of (envelope) solitary waves. Peter has also initiated research work to better understand and model the ocean mixing that is governed by ocean surface waves.

Peter is presently leading innovative model developments at ECMWF on the full interactions between waves and ocean circulation. Waves are an essential contributor to upper-ocean mixing and momentum transfer at the air-sea interface but the balance of the different processes is delicate. His highly insightful knowledge has already proven to be determinant in the release of the first operational

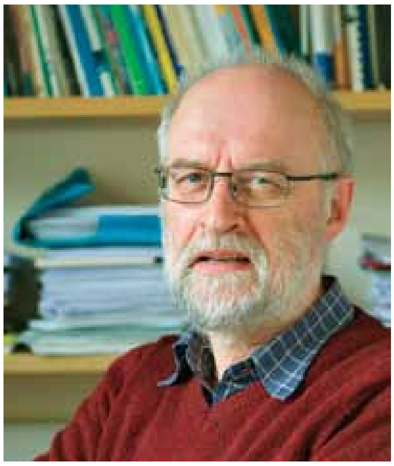

implementation at ECMWF of a model that fully couples atmosphere, surface waves and ocean.

Overall, Peter's professional contributions span a notably broad range of scientific and environmental modelling applications in forecasting of marine winds and waves. His highly insightful knowledge of the fundamentals of geophysical fluid dynamics in the ocean and atmosphere has provided a substantial basis for his successful developments of the world-leading forecasting system in operation at ECMWF.

Peter will receive the medal at the EGU 2015 General Assembly, which will take place in Vienna from 12 to 17 April 2015.

MACC-III forecasts the impact of Bardarbunga volcanic SO_2

RICHARD ENGELEN[1],
JOHANNES FLEMMING[1],
HARALD FLENTJE[2],
STEFAN GILGE[2],
VINCENT-HENRI PEUCH[1],
MIHA RAZINGER[1]
1: ECMWF
2: DWD, Hohenpeißenberg Observatory

In the middle of September 2014 several European countries experienced high concentrations of sulphur dioxide (SO_2) at ground level. SO_2 is a main contributor to winter-smog, causes acid rain and is a precursor of aerosol particles. Due to strong European efforts over the last decades to reduce SO_2 emissions, high concentrations of SO_2 are now quite rare in Western Europe – except in specific areas affected by industrial or shipping emissions. So what was going on?

French in-situ air quality stations observed high values of SO_2, especially along the northwestern coast. However, the hypothesis that these high values could be linked to ship emissions trapped in the lower atmosphere appeared unlikely because they were exceptionally high and observations in the United Kingdom, the Netherlands and Germany also showed high concentrations between 21 and 25 September. This all pointed towards an episode of large spatial extent.

The situation was explained by forecasts produced by the MACC-III (Monitoring Atmospheric Composition and Climate) project. This near-real-time forecasting system uses satellite observations to constrain the model forecasts.

The OMI instrument on board the Aura satellite provided information about concentrations of volcanic SO_2 emitted by the Icelandic Bardarbunga volcano on 20 September; these observations were assimilated by the MACC system. As shown by the chart of total column SO_2, the subsequent forecasts then captured the transport of this plume of volcanic SO_2 southward spreading over the continent on 21 and 22 September. The plume stretched all the way from Finland through Poland, Germany and France, to southern England. A parallel forecast, for which no OMI data was used, further identified the volcanic nature of the plume. No increased SO_2 values were forecast without assimilating the OMI data, which means that 'normal' emissions of SO_2 (including shipping and industrial activities) could hardly explain the observed situation.

The high SO_2 concentrations were also observed at the Hohenpeißenberg station of the Deutscher Wetterdienst (DWD), as can be seen in the plotted time series. Also shown in the same plot is the MACC-III forecast of total column SO_2 in Dobson Units. While the timing of the forecast plume is slightly too early, the skill of this forecast is remarkable. The forecast plume was not caused by actual volcanic emissions in the model, but purely by assimilating satellite data. Without assimilation of this satellite data the volcanic SO_2 plume could not have been forecast.

In the end, the French authorities used the output from the MACC global assimilation and forecasting system to assess the situation and decide what measures could be implemented locally to reduce emissions. Knowledge that the high SO_2 values were coming from the Bardarbunga in Iceland and would only be temporary helped the French authorities make an informed decision.

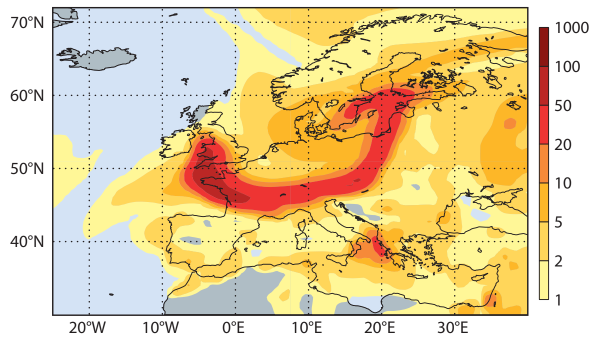

Nine-hour forecast of total column SO_2. The forecast starting from 00 UTC on 22 September 2014 shows clearly the extent of the plume of volcanic SO_2 emitted by the Icelandic Bardarbunga volcano. The volcanic SO_2 plume was initialized by assimilating OMI observations over Iceland on 20 September. The units are 10^{15} molecules/cm^2.

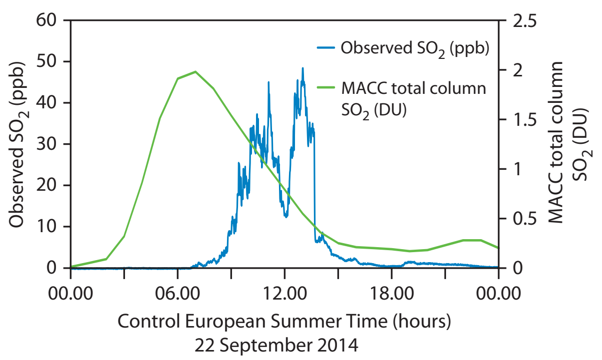

Observed and forecast concentrations of SO_2. Shown are the observed SO_2 concentration at the Hohenpeißenberg station in Germany provided by DWD and the MACC-III forecast of total column SO_2. The timing of the forecast plume is slightly too early, but the skill of the forecast is remarkable as it was based on the assimilation of satellite data rather than volcanic emissions being in the model.

ERA-20C goes public for 1900–2010

PAUL POLI, HANS HERSBACH, DICK DEE, PAUL BERRISFORD, MANUEL FUENTES, JUAN JOSE DOMINGUEZ, MATTHEW MANOUSSAKIS

The first ECMWF reanalysis of the 20th century, ERA-20C, was released on 1 October 2014. Covering the time period January 1900 to December 2010, three-hourly products describe the spatial and temporal evolution of the atmosphere, land surface and ocean waves. ERA-20C is an outcome of the ERA-CLIM project, which is funded through the EU's 7th Framework Programme for Research and Technological Development.

Production for ERA-20C was conducted in two phases.

- A first phase, between December 2012 and June 2013, involved a ten-member ensemble reanalysis (see *ECMWF Newsletter No. 139*, 15–21).
- A second phase, between December 2013 and February 2014, involved a single-member (or deterministic) reanalysis.

The second phase applied lessons learnt from the first, correcting several problems therein (see ERA Report Series 14 for details). All productions were conducted on ECMWF's IBM Power7, with an average yield of 3.5 Tb/day, and about 2,500 data assimilations run daily.

The second production phase was the fastest of all atmospheric reanalysis productions ever conducted at ECMWF, with 130+ years of reanalysis products, spread over 22 six-year-long streams, generated in under two months. Fifteen years after the introduction of four-dimensional data assimilation (4D-Var) at ECMWF, these productions represent the first large-scale applications of that technique for such long time periods. More about ECMWF reanalyses can be found at http://www.ecmwf.int/en/research/climate-reanalysis.

The first year of each production stream was used for spin-up. The final released product excludes these spin-up years. Data from multiple streams was consolidated following an updated procedure which checks for continuity of the archive over time and verifies that not a single field is missing. In addition, the actual data values are checked against the original streams for several randomly chosen months.

The ERA-20C data server (http://apps.ecmwf.int/datasets/data/era20c_daily) provides an interface similar to that of ERA-Interim. Users can select parameters and time periods of interest for download. For large retrievals, scripts are available to download data in batch mode. The data can be freely used for applications, including commercial ones, under conditions set out at http://apps.ecmwf.int/datasets/data/era20c_daily/licence/.

This reanalysis represents the first efforts at ECMWF to explicitly account for time-varying error conditions in reanalysis, as the observing networks evolved with human history. Between 1900 and 2010, there is, for example, a factor 50 increase in the number of daily observations of surface pressure. This is reflected by much better synoptic weather charts in ERA-20C near the end of the century than at the beginning, and gradually reduced weight given to observations as compared to background.

When users obtain the data and provide feedback or publish their findings, they will help improve the way future reanalyses are produced, thereby benefiting climate research and societal applications.

ERA-20C output and production

The products from ERA-20C describe the atmosphere on 91 vertical levels (between the surface and 0.01 hPa), 4 land-surface soil layers, and the ocean waves (25 frequencies and 12 directions). The product horizontal resolution is approximately 125 km (spectral truncation T159). The atmospheric products are not only available on the native 91 model levels, but also on 37 pressure levels (as in ERA-Interim), 16 potential temperature levels, and the 2 PVU potential vorticity level.

ERA-20C uses the same coupled Atmosphere/Land-surface/Ocean-waves model version (Cy38r1 of the Integrated Forecasting System) and surface and atmospheric forcings as the final version of the atmospheric model integration ERA-20CM (*ECMWF Newsletter No. 139*, 15–21). The assimilation methodology is 24-hour 4D-Var analysis with variational bias correction of surface pressure observations. Analysis increments are at T95 horizontal resolution (approx. 210 km). The analyses provide the initial conditions for subsequent forecasts that serve as backgrounds to the next analyses. A ten-member ensemble was produced initially to estimate the spatio-temporal evolution of the background errors.

The observations assimilated in ERA-20C include surface and mean sea level pressures from the International Surface Pressure Databank (ISPDv3.2.6), and surface marine winds from the International Comprehensive Ocean-Atmosphere Data Set (ICOADSv2.5.1). The observation feedback from ERA-20C, including, for example, observation innovations and residuals and usage flags, is due for public release.

Use of high-performance computing in meteorology

PETER TOWERS

Every second year ECMWF hosts a workshop on the use of high-performance computing in meteorology. The 16th workshop in this series took place from 27 to 31 October 2014 and was attended by over 80 participants from meteorological services, research institutions and computer vendors, coming from 18 countries. High-performance computer architectures are becoming ever more complex, which presents significant challenges for the continuing development of operational meteorological applications. The workshop examined the issues surrounding the scalability of NWP codes and the steps that will be required to enable the use of future large-scale heterogeneous computer systems.

At the workshop there were 46 presentations covering a wide range of topics, including:

- High-performance computing at various forecasting centres.
- Current and future products from vendors of supercomputers.
- Developments in parallel computing techniques.
- Tools to exploit the power of supercomputers.

The keynote talk was given by Dr Venkatramani Balaji from Princeton University, who also heads the Modelling Services team of the Geophysical Fluid Dynamics Group at the NOAA Office. He presented the trends in climate science driving models toward higher resolution, greater

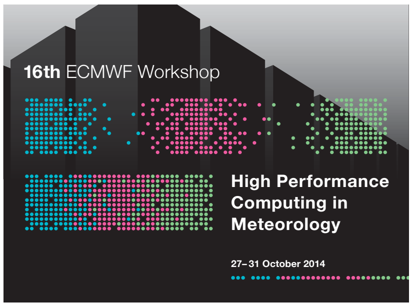

complexity, and larger ensembles, all of which present computing challenges. He also discussed the prospects for adapting these models to novel hardware and programming models.

Presentations from this workshop can be found at: http://www.ecmwf.int/en/workshop-high-performance-computing-meteorology

Exploring the potential of using satellite data assimilation in hydrological forecasts

BOB RIDDAWAY

Combined workshops on H-SAF (EUMETSAT Satellite Application Facility on Support to Operational Hydrology and Water Management) and HEPEX (Hydrological Ensemble Prediction Experiment) were held at ECMWF from 3 to 7 November. These workshops brought together experts in hydrological product development, satellite data assimilation and hydrological forecasting from both research and operational centres.

H-SAF aims to develop, deliver and validate operational satellite-derived products of precipitation, snow and soil moisture. The workshop put the emphasis on having a better implementation of satellite products in NWP systems and hydrological models. The H-SAF workshop:

- Reviewed the status of hydrological variables, retrieval algorithms and to exchange information and ideas on innovative approaches to prepare future satellites (e.g. GPM and NPOESS).
- Characterised the accuracy of hydrological products and discuss the validation metrics.
- Reviewed the status of activities on model optimisation and hydrological products data assimilation and to discuss the impact of products on hydrological models.
- Promoted the use of H-SAF products and attract interest for expanding the user community during CDOP-2 phase and follow-on.

HEPEX is concentrating on key questions such as what adaptations are required for meteorological ensemble systems to be coupled with hydrological ensemble systems? How should the existing hydrological ensemble prediction systems be modified to account for all sources of uncertainty within a forecast? What is the best way for the user community to take advantage of ensemble forecasts and to make better decisions

based on them? The HEPEX workshop:

- Showcased methods in pre-processing of NWP products as input into hydrological forecasting chains (contribution to the HEPEX Scientific Implementation Plan on Pre-processing).
- Demonstrated data assimilation in operational hydro-meteorological forecasting chains (contribution to the HEPEX Scientific Implementation Plan on Data assimilation).

More information can be found at: http://www.ecmwf.int/en/h-saf-and-hepex-workshops-coupled-hydrology

New Cray High-Performance Computing Facility

MIKE HAWKINS

Phase 1 of the new Cray High-Performance Computing Facility (HPCF) completed acceptance on 29 September 2014. This follows the successful migration of the ECMWF time-critical operational suites on 17 September and marks the end of a period of intense work that began with the signing of the contract with Cray UK Ltd on 24 June 2013.

Installing a new HPCF is a far from straightforward affair. Before installing the system, the computer halls had to be prepared. Each cluster needs an electrical distribution system to deliver 1.2 megawatts of power, enough to run 6,000 UK homes, and a water cooling system delivering 40 litres per second, the equivalent of 150 domestic showers. Cray completed the preparation of the computer halls ahead of schedule and delivered the first cluster, which was built to order, to ECMWF on 6 November 2013; it came in 53 very large crates and took 12 people two days to install.

In parallel with the physical installation, there was the migration of the Integrated Forecasting System (IFS) and all of the associated software. Work on this started on a remote system provided by Cray in early July 2013 and stepped up in mid-August with the delivery to ECMWF of a small training system. The work then went into high gear when the initial group of early users were allowed on to the first of the main systems on 6 December. This sustained effort from many people across the Centre led to the successful migration of the operational suites on 17 September 2014. Although the operational forecast production has been successfully migrated to the Cray platform, efforts are ongoing as there is a lot of work still needed to optimise the IFS for the new system so that we get the best out of it. This is particularly true for the way the applications read and write files to the Lustre high-performance storage system.

Celebrating the successful migration of the operational suites to the new Cray HPCF. Mike Hawkins (ECMWF), Peter Bauer (ECMWF), Erland Källén (ECMWF), Anne Glover (European Commission), Fiona Burgess (Cray UK Ltd), Alan Thorpe (ECMWF), Rob Varley (Met Office, UK), Peg Williams (Cray Inc, USA), Florence Rabier (ECMWF), Nyall Farrell (ECMWF), Adrian Wander (ECMWF) and Isabella Weger (ECMWF).

The ECMWF acceptance test process is necessarily lengthy due to site power restrictions and the need to maintain an operational service. There is only enough power and cooling capacity on-site to run three clusters of the size used in our HPCF. This means that one cluster of the new system is installed alongside the two clusters of the old HPCF. When the new cluster is accepted and is shown to be able to run the IFS properly, one of the clusters of the old HPCF can be powered down. This allows the installation and acceptance testing of the second cluster of the new system.

The two clusters of the Cray HPCF provide ECMWF with about three times the performance of the previous HPCF. Each cluster consists of 19 Cray XC30 cabinets equipped with Intel Ivy Bridge processors, providing around 3,500 dual-socket compute nodes per cluster, connected by the Cray 'Aries' proprietary high-performance interconnect network. In order to achieve the number of floating point operations (e.g. the addition or multiplication of two numbers) that this system is capable of every second, the entire population of the UK would need to work flat out for just under two years. The interconnect networks within the system, which provide a powerful communication infrastructure for running ECMWF's numerical weather models, have sufficient bandwidth to move the equivalent of over 90 million simultaneous high-definition video streams. Six petabytes of storage are attached to each cluster; this amount of storage is enough to hold over 1.3 billion songs in MP3 format.

The system is scheduled to be in service at ECMWF until the autumn of 2018. The new HPCF provides ECMWF with the computing power needed to implement the next major step in its strategy, namely the upgrade of the horizontal resolution for the high-resolution forecast.

Anton Beljaars elected as an AMS Fellow

XUBIN ZENG
(University of Arizona),
PETER BAUER (ECMWF)

In October 2014 the American Meteorological Society (AMS) elected 28 of its members to the prestigious rank of AMS Fellow. Anton Beljaars was included in recognition of his fundamental contributions to the observation, understanding and model parametrizations of atmospheric turbulence, and land and ocean surface processes.

As Principal Scientist and Head of the Physical Aspects Section, Anton has played a major role in developing parametrization of atmospheric and surface processes used in ECMWF's Integrated Forecasting System (IFS). In particular, he has developed new ideas about turbulence under very stable and unstable conditions and the interaction between turbulence and land surfaces. These insights enabled him to develop improved turbulence parametrizations that are widely used.

Anton has played a major role in international research programmes. His studies of land–surface interactions provided one of the scientific underpinnings for the success of GEWEX (Global Energy and Water Exchange Experiment). Also, Anton's work on ocean–atmosphere interactions inspired some aspects of TOGA-COARE (Tropical Ocean Global Atmosphere-Coupled Ocean Atmosphere Response Experiment) that brought together meteorologists and oceanographers

Due to his international reputation, Anton has served on a variety of key international committees (e.g. GEWEX Scientific Steering Group and Mission Advisory Group of the ESA Earth-CARE satellite).

The AMS has about 14,000 members from academia, government and the private sector in various countries. Each year, the Council of the AMS elects as Fellows no more than 1 of every 500 of the Society's members. Fellows are nominated by their peers for outstanding contributions over many years to the atmospheric and related oceanic and hydrologic sciences and applications.

The new Fellows will be honoured formally in January 2015 at the 95th AMS Annual Meeting in Phoenix, Arizona.

Decisions, decisions…!

TIM PALMER (University of Oxford),
DAVID RICHARDSON (ECMWF)

"Forecasts possess no intrinsic value. They acquire value through their ability to influence the decisions made by users of the forecasts" (Allan Murphy)

As indicated by the quote above, the sole purpose of making weather forecasts is to aid decision-making. As a daily commuter, should I take my umbrella to work? As a regional governor, should I order the evacuation of a coastal city ahead of some possible hurricane? As an aid worker, should I prepare for relief measures ahead of an ongoing drought? But are forecasts any good for aiding these types of decisions? If we think that they are, how would we actually go about measuring this quantitatively?

In this note, we outline the reasons why one of ECMWF's principal headline scores – the continuous ranked probability skill score (CRPSS) – is just such a measure. For many readers this might come as a surprise; when defined explicitly, the CRPSS looks like a rather arcane probabilistic skill score which only ensemble-forecast experts are able to understand well.

The continuous ranked probability score (CRPS) compares the forecast probability distribution of a quantity to its analysed value. Both forecast and analysis are expressed as cumulative distribution functions. The CRPS is the squared difference between these distributions, integrated over the range of the quantity being assessed. The CRPSS then compares CRPS of the verified forecast to that of a reference unskilled forecast.

However, it turns out that the CRPSS has a direct and very practical interpretation in terms of decision-making. This is due to the work of Allan Murphy, professor at Oregon State University, who was a pioneer in the field of probabilistic weather forecast verification and devised methods for assessing the value of probabilistic weather forecasts (Allan died in 1997).

To see how to interpret CRPSS we need to discuss how we might go about measuring the value of weather forecasts. To do this, it makes sense to try to generalise and idealise the examples given above, so that the notion of value can be discussed independent of the minutiae of the practical details which are important in individual real-world situations.

Hence, imagine a hypothetical user of weather forecasts, who stands to make a loss L if some adverse weather event occurs (e.g. freezing temperatures, winds exceeding a given speed, rain exceeding some chosen threshold). The loss need not be purely monetary – in the examples related to disaster mitigation and relief, the loss includes human suffering. However, in order to define a quantitative measure of value we have to assume that L can, in principle, be given a numerical value. We will also assume that the user can take precautionary action at cost C to avoid these losses. If the user is the regional governor in the example above, then C denotes the cost of evacuation.

When should such precautionary action be taken?

If L is sensitive to weather, then a good weather forecast is clearly of value in deciding whether or not to take action. However, we need a strategy on how to use the weather forecast for such decisions. A particularly simple strategy might be this: take precautionary action if the forecast predicts the event will occur. This strategy makes sense if the user only has available a single deterministic forecast. However, if the user is an ECMWF customer, then another (generally superior) decision strategy is available.

In economic language, the risk associated with some event is equal to the probability p of that event occurring multiplied by the damage L associated with that event. The ECMWF ensemble forecast (ENS) allows users to directly estimate this all-important probability, without which a proper assessment of risk is impossible. If ENS estimates that the event will occur with probability p (which means that the frequency of occurrence of the event in ENS, at the relevant lead time, equals p), then the risk of the event is equal to pL. The superior strategy referred to above is to take precautionary action when the risk pL exceeds C. Put another way, the strategy is to take precautionary action if the forecast probability of the event exceeds C/L. To make this more concrete, suppose the cost C of precautionary action is one tenth of the unmitigated loss L if the weather event occurs (so that $C/L = 0.1$), then the user should take precautionary action when the forecast probability of the event, according to ENS, exceeds 0.1.

Now if users were to pursue either of these decision strategies, they could assess, let us say after a season of forecasts, whether the forecasts were valuable in making decisions. How are we to measure value? Rather than present value in euros, dollars or pounds, we can measure value by comparison with two standard benchmarks.

- An upper bound on value is associated with that of a hypothetical oracle. This hypothetical oracle can, by definition, forecast the weather perfectly. If one had access to the oracle, one would take precautionary action only when the oracle said the weather event will occur. We will assign a normalised value of 1 to this perfect hypothetical oracle.
- A lower bound on value is associated with knowledge of the climatological frequency, p_c of the weather event of interest. A decision strategy based on a knowledge of p_c alone, is to take precautionary action when $C/L<p_c$. In this (low-value) strategy, one should always take precautionary action if the cost is sufficiently cheap compared to the potential loss, and never take preventative action if the cost is sufficiently high. We will assign a normalised value of 0 to this 'climatological' decision strategy.

We can calculate a corresponding normalised value for the ECMWF forecasts – we call this the 'potential economic value'. The potential economic value of ECMWF forecasts can never be greater than 1; hopefully it will be greater than 0. If it is less than 0, a user should instead base decisions on the climatological strategy mentioned above. The user can readily convert from this normalised measure to financial value: if they know the financial benefit that a perfect forecasting system would bring, the potential economic value shows what fraction of this would be realised by the available forecasting system.

Figure 1 compares the potential economic value of decision strategies based on the ENS and ECMWF's high-resolution forecast (HRES). The x-axis in Figure 1 describes the user cost-loss ratio (C/L), and the y-axis describes the normalised potential economic value. It can be seen that ENS has greater value than HRES for all cost-loss ratios. What may be

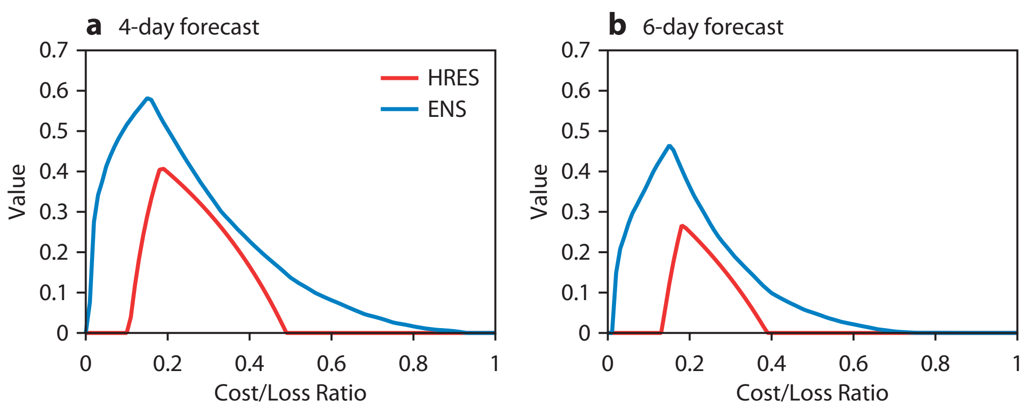

Figure 1 Potential economic value of the high-resolution forecast (HRES) and the ensemble forecast (ENS) in predicting 24-hour precipitation amounts greater than 5 mm over Europe for the summer (June to August) 2014: (a) four-day forecast and (b) six-day forecast.

surprising is that HRES has no value (over decisions made with climatological information only) for users with either high or low cost-loss ratios. This means that decisions using the climatological strategy are superior to those using HRES, for low and high cost-loss ratios. The ENS is valuable for a much larger range of users than the HRES.

Note that the value of HRES can be improved by 'dressing' it using a probability distribution function based on climatological errors. However, ENS is still superior to this dressed HRES in the medium range, and ENS can be further improved by statistical calibration of the ensemble itself, *Gneiting* (2014).

Let us denote by $\overline{V}$ the average potential economic value of ENS overall cost-loss ratios between 0 and 1. As shown by *Murphy* (1966), $\overline{V}$ is equal to a standard skill score for evaluating probability forecasts called the Brier Skill Score.

But we can go further. So far we have imagined decisions based on the occurrence of a particular weather event. For the sake of argument, let us suppose that this event is associated with the daily rainfall total exceeding some threshold T_0 (Figure 1 shows the results for $T_0 = 5$ mm). The Brier Skill Score depends on the choice of threshold T_0. However, we can ask what is the average Brier Skill Score as T_0 varies across all values of threshold, where the average is weighted with the climatological probability of occurrence of T_0. Such an averaged Brier Skill Score is none other than the CPRSS.

So, putting all this together, the CRPSS is simply a normalised measure of the potential economic value of a forecast system (typically an ensemble forecasting system) for a family of users which span the possible range of cost-loss ratios and for weather events which span the range of possible rainfall thresholds. That is to say, CRPSS is perhaps the simplest single measure of the overall value of a forecasting system for decision-making!

By contrast, the traditional Anomaly Correlation Coefficient (ACC) of say the 500 hPa height cannot be directly related

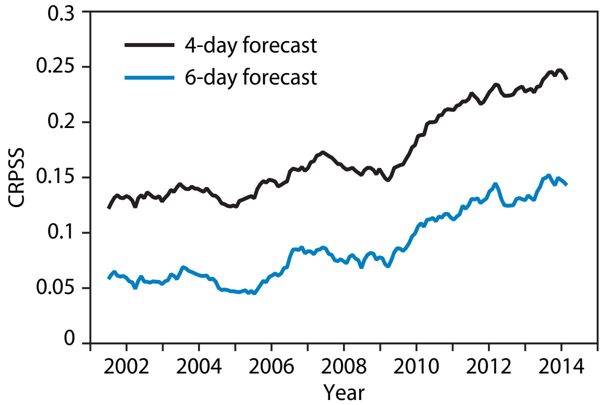

Figure 2 CRPSS for ENS probabilistic precipitation forecasts at day 4 and day 6 over Europe. Each curve is a centred 12-month mean.

to decision strategies in this way. ECMWF's set of headline scores and the wide range of additional evaluation measures provide essential feedback to both users and model developers on the quality of the forecasting system. Together, they assess the underlying quality of the forecasting system as well as the potential benefits to users.

Insofar as the primary metrics of forecast quality should reflect their use in the real world, CRPSS is a much more relevant metric than ACC. As such, CRPSS deserves to have much higher visibility amongst ECMWF's customers than it currently does! Hence, to close, we show a timeseries of CRPSS for the ENS (Figure 2). The ENS skill has improved substantially over the years. More directly, in the language of the simple economic decision-making framework that we have used in this note, the potential economic value of the ECMWF ensemble has doubled over the last 15 years. In this idealised framework, if a perfect forecasting system (the oracle) would save the European economy €100 billion, then a forecasting system with a CRPSS of 0.2 would realise €20 billion of this saving. Doubling the CRPSS from 0.1 to 0.2 means doubling the savings from €10 billion to €20 billion.

FURTHER READING

The quote at the beginning of this note is from an article by Alan Murphy published in 1993 entitled "What Is a Good Forecast? An Essay on the Nature of Goodness in Weather Forecasting" (*Wea. Forecasting*, **8**, 281–293).

The potential economic value shown in Figure 1 is regularly updated on the ECMWF web site, as are the CRPSS headline scores for the ENS. For these and other routine verification see: http://www.ecmwf.int/en/forecasts/tools-and-guidance/quality-our-forecasts

For more information on the cost-loss model and the potential economic value of the ECMWF ensemble (including limitations and extensions) see:

Murphy, **A.H.**, 1966: A note on the utility of probabilistic predictions and the probability score in the cost-loss ratio decision situation. *J. Appl. Meteorol.*, **5**, 534–537.

Richardson, **D.S.**, 2012: Economic value and skill. In *Forecast Verification: a Practitioner's Guide in Atmospheric Science (2nd edition)*, Jolliffe, I.T. and Stephenson, D.B., Eds., Wiley, 249 pp.

Richardson, **D.S.**, 2001: Measures of skill and value of ensemble prediction systems, their interrelationship and the effect of ensemble size. *Q. J. R. Meteorol. Soc.*, **127**, 2473–2489.

Richardson, **D.S.**, 2000. Skill and relative economic value of the ECMWF Ensemble Prediction System. *Q. J. R. Meteorol. Soc.*, **126**, 649–668.

Calibration of ensemble forecasts is reviewed in:

Gneiting, **T.**, 2014: Calibration of medium-range weather forecasts. *ECMWF Tech. Memo. No. 719.* http://old.ecmwf.int/publications/library/do/references/show?id=91014

Towards predicting high-impact freezing rain events

RICHARD FORBES, IVAN TSONEVSKY, TIM HEWSON, MARTIN LEUTBECHER

The term 'freezing rain' usually refers to the occurrence of supercooled rain drops falling onto a sub-freezing surface. The drops freeze on impact and can result in a glaze of ice, coating any objects that are below 0ºC, such as power lines, trees and road surfaces. When the precipitation is heavy and/or prolonged (sometimes referred to as an 'ice storm') the consequences can be severe, with disruption to air and ground transport, an increase in road accidents and hospital admissions, power loss due to collapsing power lines, and significant damage to infrastructure and vegetation (*Call*, 2010) – see Figure 1.

Such extreme events are fortunately rare, but freezing rain and drizzle are not uncommon during the winter months over Europe and North America and prediction of such high-impact weather is vital. A typical location is ahead of a surface warm front where an elevated layer of warm air is forced over a surface layer of very cold continental or Arctic air. If embedded in deep frontal cloud, snow particles melt in the warm elevated layer to form rain drops which then remain as supercooled liquid as they continue to fall into the sub-freezing near-surface layer below, until freezing on impact at the surface.

In the ECMWF Integrated Forecasting System (IFS) cycle 41r1, to be operational in early 2015, there are changes to the cloud and precipitation physics that allow an improved prediction of freezing rain. To this end a new 'precipitation type' diagnostic is added which includes the freezing rain category described here. In addition, there are new diagnostics for convective/stratiform precipitation rates valid at a particular time (rather than averaged or accumulated over a period) which are consistent with the precipitation type diagnostic.

A first evaluation of the freezing rain precipitation type as an experimental product shows promise for providing advance warning of severe freezing rain events. However, more experience needs to be gained over the coming winter and further evaluation of the probability of freezing rain in medium-range ensemble forecasts is required.

Freezing rain events

Figure 2 shows schematics of the vertical structure of temperature and precipitation type for four scenarios, each of which is associated with a different precipitation type at the surface. Figures 2a and 2b represent relatively straightforward situations in which the surface precipitation type is, respectively, snow and a rain/snow mix in the melting layer. The former scenario arises when temperatures are sub-zero at all levels, and the latter when

Figure 1 The impacts on transport, power lines and forest damage due to a severe freezing rain event in Slovenia in early February 2014. (Acknowledgements: top left/right and bottom left - Srdjan Zivulovic/Reuters, bottom right - Marko Korosec/Solent News).

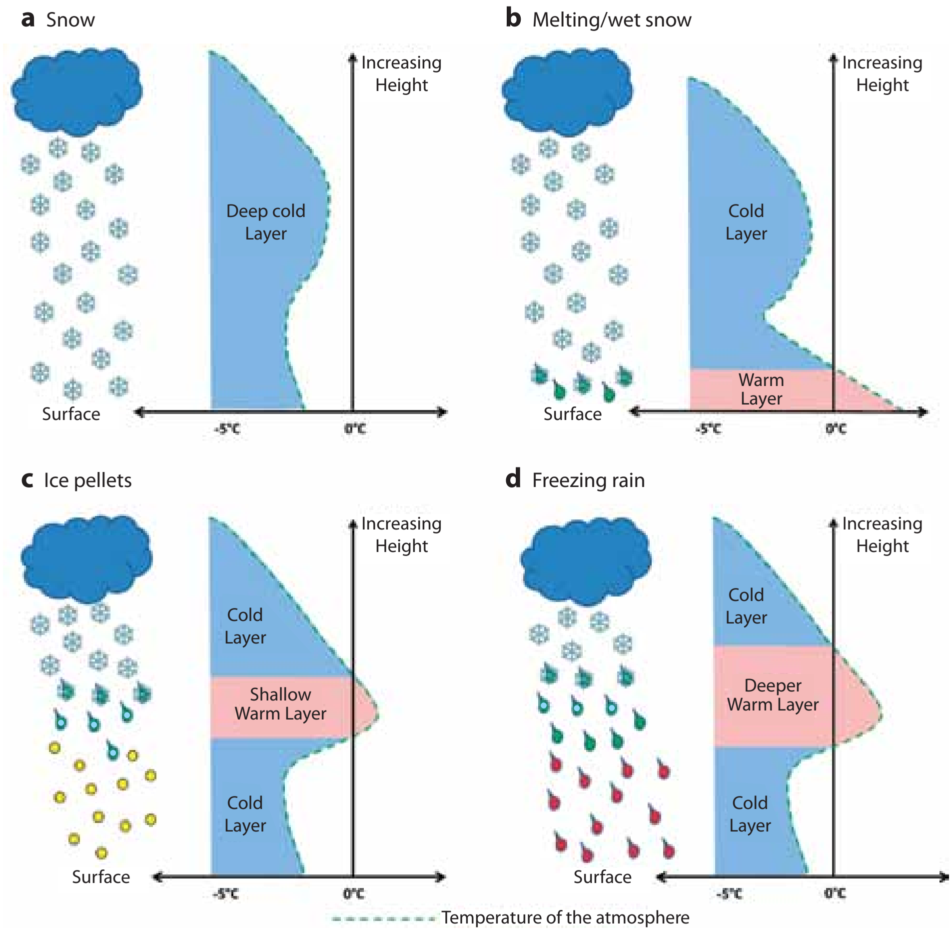

Figure 2 Schematic of typical temperature profiles for different precipitation types: (a) snow, (b) melting/wet snow, (c) ice pellets and (d) freezing rain (all assuming 100% relative humidity).

the freezing level is near the surface. The more complex scenarios in Figures 2c and 2d show an elevated warm layer with a sub-freezing layer below. In this case, ice pellets or freezing rain can occur. As a snow particle falls into the elevated warm layer it will start to melt and will keep falling as the melting process continues. If the snow particle does not completely melt before it reaches the layer of sub-freezing temperatures, it will still contain an ice core. This acts as an ice nucleus and facilitates rapid freezing of the whole particle, forming a denser more homogeneous ice particle called an ice pellet.

However, if the snow particle has completely melted when it reaches the sub-freezing layer it will remain as a supercooled drop. If the air is only a few degrees below freezing near the surface, it may not be cold enough for heterogeneous freezing of the drop and it will reach the surface as supercooled water. Only if the near-surface cold layer is particularly cold and deep is refreezing likely to occur due to impurities in the drop acting as potential ice nuclei. Thus the melting process and the depth and temperature of the sub-freezing layer are all key to the formation of freezing rain at the surface, as discussed by *Czys et al*. (1996).

Freezing rain events typically occur during winter where a sub-tropical or maritime warm air mass meets a cold Arctic or continental air mass, often ahead of a warm front. The wind profile changing with height leads to advection of a warm layer above a sub-freezing layer near the surface. Such regions can cover many hundreds of kilometres with precipitation type changing perpendicular to the front from rain to freezing rain (Figure 2d) and then to snow (Figure 2a). Sometimes there is a narrow band of ice pellets in-between the freezing rain and the snow (Figure 2c) at the shallow end of the elevated warm layer.

Carrière et al. (2000) describe a climatological study of surface freezing precipitation from SYNOP messages over Europe during three winters from 1995 to 1998. They found freezing precipitation is most frequent during the months of December to February and when near-surface temperatures are between -5ºC and 0ºC. Freezing rain and freezing drizzle were observed in up to 1% of the SYNOP reports during this period, commonly occurring in regions where the climate is more continental, over Germany and Central Europe. Ice pellets were relatively rarely observed. The most frequent mechanism for freezing precipitation formation was snow melting in an elevated warm layer and refreezing below. A second mechanism in which the collision-coalescence process in supercooled liquid water cloud produces freezing drizzle also occurred relatively frequently.

Representing precipitation type in the IFS

To be able to predict the correct precipitation type at the surface, including freezing rain, an atmospheric model needs to predict the vertical temperature profile and the amount of precipitation sufficiently accurately, but must also clearly include the correct physics for the melting and refreezing processes. Since the major upgrade to the IFS cloud scheme in the operational model in November 2010 (IFS cycle 36r4), rain and snow have been represented as separate prognostic variables, with parametrizations of snow melting for wet-bulb temperatures greater than 0ºC, rain freezing for temperatures below 0ºC, and precipitation evaporation. So for the case of a freezing rain temperature profile with this model physics, the snow melts in the warm air and then rapidly refreezes in the low-level sub-freezing layer, reaching the ground as snow. Thus the processes that lead to freezing rain at the surface are not adequately represented.

In the new version of the cloud and precipitation parametrization, the freezing rain process for elevated warm layers is modified. It includes a more representative timescale for the refreezing of rain drops which depends on the temperature and crucially on whether the snow particles have completely melted or not (*Zerr*, 1997).

- If most of the snow particles have completely melted by the time they reach the base of the warm layer aloft, the refreezing process is slow and supercooled rain at the surface is diagnosed.
- If the majority of snow particles have not completely melted in the warm layer aloft, then refreezing is rapid and a precipitation type of ice pellets is diagnosed at the surface.

Whether the precipitation refreezes or not in the cold air below also affects the temperature profile, resulting in colder temperatures in the layer if the particles remain as supercooled water. The latent heat of fusion is instead transferred to the surface with the rain freezing on impact and a relative warming of the surface and near-surface temperature.

In the IFS model the melting and refreezing parametrizations must be formulated in terms of the two prognostic variables for precipitation: rain and snow. The precipitation type (rain, snow, freezing rain, ice pellets, wet snow or mixed rain/snow) is diagnosed from the ratio of rain and snow at the surface and the profile of precipitation and temperature above (see Box A for more detail). Note that although the physics of melting and refreezing allow the prediction of supercooled rain at the surface, the generation of drizzle particles from supercooled liquid water cloud, when there is no warm layer,

Parametrization of the physics of supercooled rain formation

A

The melting and refreezing of precipitation particles are the key physical processes for the formation of freezing rain. The parametrization of these processes in the IFS is briefly described below.

Melting process

The rate of snow melting can be determined using thermal heat balance, considering the latent heat due to the melting of a snow particle (latent heat of fusion) and the latent heat due to vapour transfer from the particle into the atmosphere (sublimation). Integrating over an assumed particle size spectrum gives a melting rate that is proportional to the wet-bulb temperature difference from 0ºC. The complexities of the physics at the microscale and wide range of particle sizes can be represented more simply with an effective melting timescale.

The melting process is parametrized in the IFS by allowing a grid box containing precipitating snow to cool towards a wet-bulb temperature of 0ºC through the latent heat of melting over a timescale τ:

$$\text{Melting rate} = -\frac{C_p}{L_{fus}}\left(\frac{T_w - T_0}{\tau}\right)$$

where C_p is the specific heat capacity of water, L_{fus} is the latent heat of fusion (melting), T_w is the wet-bulb temperature of the air in degrees Celsius, and T_0 equals 0ºC.

This parametrization captures the essential dependency on the temperature difference from 0ºC, the effect of evaporative cooling in subsaturated air through the use of wet-bulb temperature, and the depth of the melting layer through the relaxation timescale. The melting parametrization is the same as in the current operational forecasts which determines whether surface precipitation is rain, snow or mixed when the temperature is close to 0ºC.

Refreezing process

If the warm layer is shallow and the majority of the rain drops still contain an ice core, then they will refreeze rapidly when entering the sub-freezing layer below. The refreezing rate (transfer of mass from the rain category to the snow category) is uncertain, but for now it is parametrized with the same functional form and timescale as the melting rate described above. It is assumed at least 20% of the precipitation mass must be in the ice phase at the base of the elevated warm layer for refreezing to be rapid, otherwise the majority of rain drops are assumed to not contain an ice core and refreezing will occur at a much slower rate through heterogeneous ice nucleation. In the latter case an order of magnitude longer timescale is used for the refreezing rate, so the supercooled rain can still refreeze before reaching the surface if the near-surface subfreezing layer is very cold and/or deep.

Freezing rain is diagnosed if the 2-metre temperature is below 0ºC, at least 80% of the precipitation mass is in the liquid phase at the base of the elevated warm layer and at least 20% remains as supercooled rain when it reaches the surface. Ice pellets are diagnosed if the percentage of precipitation mass in the ice phase at the base of the warm layer is between 20% and 80%, otherwise the precipitation is classed as snow. In regions of freezing rain, the reduced refreezing in the new physics leads to a relative cooling of the lower-tropospheric air mass (less heating) and warming of the surface and near-surface temperature because the latent heat released during refreezing is instead transferred to the surface.

Clearly the form of the melting and freezing rate parametrizations and choice of thresholds are a significant simplification of many complex processes that could be improved in the future. However, this describes an initial implementation that captures the first order characteristics of the precipitation melting and refreezing processes.

is not yet represented. Supercooled drizzle drops resulting in 'freezing drizzle' at the surface, although not as severe as heavy freezing rain events, is still an important forecasting issue and will be addressed in the future.

Evaluation of IFS freezing rain prediction: case studies

A case study of a severe freezing rain event over Slovenia, Croatia and surrounding areas in early February 2014 is used to illustrate the potential for the IFS to predict such events. Another example from December 2013 over North America is also described.

Case study 1: February 2014, Slovenia

Heavy snow and freezing rain affected Slovenia and the surrounding region over several days from 31 January to 5 February 2014 with widespread accumulations of 10 to 50 mm and locally above 100 mm. The worst affected area was the south-western region of the country, especially around the city of Postojna. During the event, the freezing rain coated all surfaces in a thick layer of ice (photos of this event have already been shown in Figure 1). There were reports of more than 300 broken power lines and 25% of Slovenian residents were without electricity, heating and water. It was also estimated that 40% of Alpine forests were destroyed by the weight of ice accumulation on the trees.

Figure 3 shows the synoptic situation at 00 UTC on 2 February with an occluded front over northern Italy, Slovenia and Croatia, marking the boundary where cold continental air could be undercutting the warmer air to the south, giving a situation where freezing rain is possible. A second occluded front is present to the north, through Germany and across the Baltic Sea to southern Sweden, which moved eastward through the day. Also shown is the sounding from Ljubljana at 05 UTC on 2 February showing the elevated warm layer above 0ºC with winds from the south-east and the sub-freezing layer below 860 hPa with lighter winds from the north-east.

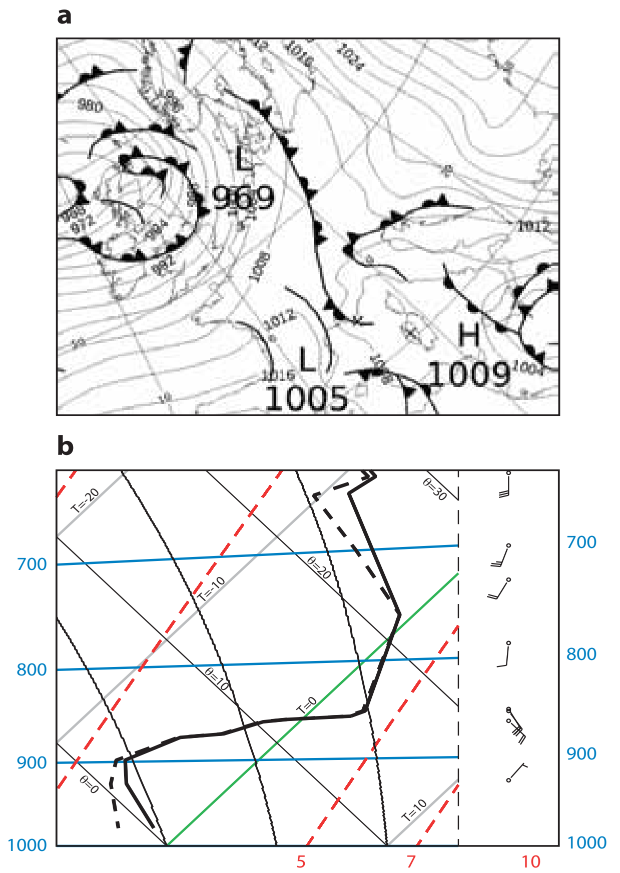

Figure 3 (a) UK Met Office analysis for 00 UTC on 2 February 2014 showing the occluded fronts over central Europe. (b) Tephigram at 05 UTC from Ljubljana in Slovenia showing the elevated warm layer above 0ºC between 780 hPa and 860 hPa with winds from the south-east and the sub-freezing layer with light winds below. The tephigram shows the temperature (solid black) and dew point temperature (dashed black) profiles and isopleths for potential temperature (θ), temperature (*T*), mixing ratio (dashed red) and pressure (blue). The 0ºC isotherm (*T*=0) is green.

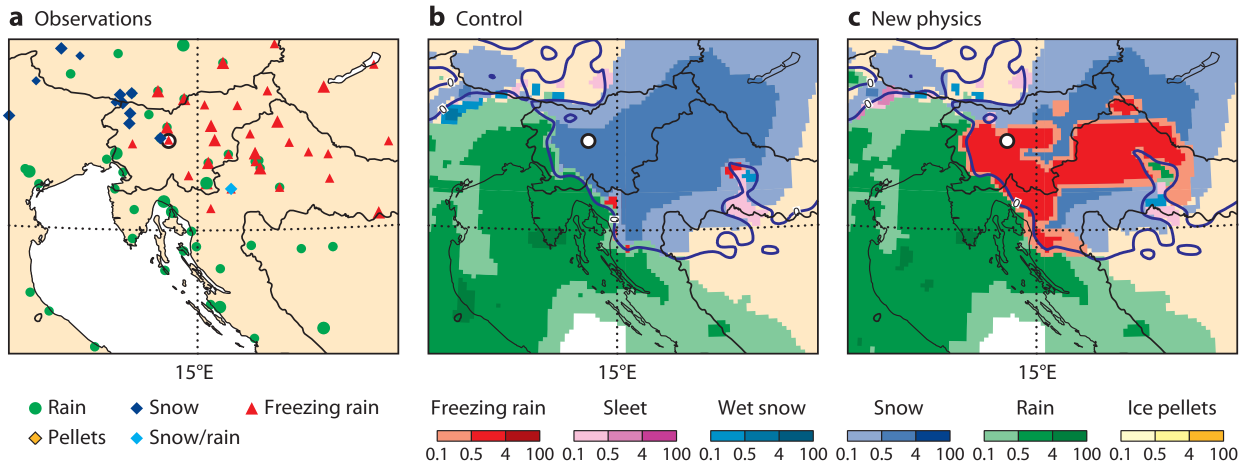

Figure 4 A significant freezing rain event occurred in Slovenia and Croatia in early February 2014. (a) The observed precipitation type from SYNOP reports at 06 and 12 UTC on 2 February 2014. (b) Precipitation rate and type from the short-range HRES initialised at 00 UTC and valid for 09 UTC for the version of the model operational at the time (i.e. the control). (c) As (b), but with the new physics. The forecast with the new physics gives a clear signal of relatively heavy freezing rain in the region of the most affected areas. Shading in (b) and (c) is for 0.1, 0.5 and 4 mm hr^{-1} and the thick blue contour is the 2-metre temperature 0ºC isotherm. The location of Ljubljana is marked with a circle.

As an example, a comparison of observed and model-predicted precipitation type for the same day during the event is shown in Figure 4. The SYNOP reports of precipitation type at 6 and 12 UTC on 2 February show widespread observations of freezing rain across Slovenia and into northern Croatia. To highlight the impact of the new physics, short-range predictions of precipitation type from the IFS high-resolution forecast (HRES) initialized at 00 UTC that morning are shown for 09 UTC for the operational model as the control (Figure 4b) and with the new physics (Figure 4c). The new precipitation type diagnostic shows that the operational model was unable to predict the extent of the freezing rain event, instead predicting widespread surface snowfall, whereas the model with the new physics is able to predict freezing rain over much of Slovenia and northern Croatia in general agreement with the observations.

Medium-range predictions are more usefully expressed in terms of the probability of freezing rain accumulation over a specified threshold. Again, focusing on the same day as an example, Figure 5a shows the observed SYNOP reports overlaid at 00, 06, 12 and 18 UTC during the 24-hour period on 2 February 2014 over a larger region of Europe.

Observations of freezing rain were quite common over central Europe, notably in a north–south orientated band crossing Poland and the Baltic States. These observations were associated with the northern occluded front seen on Figure 3a. The other panels in the figure show the probability of freezing rain for accumulations above different thresholds on 2 February 2014 for day 3 of the ensemble forecast (ENS).

For a low threshold of 0.5 mm (Figure 5b), probabilities of around 20% are predicted for the regions in central Europe,

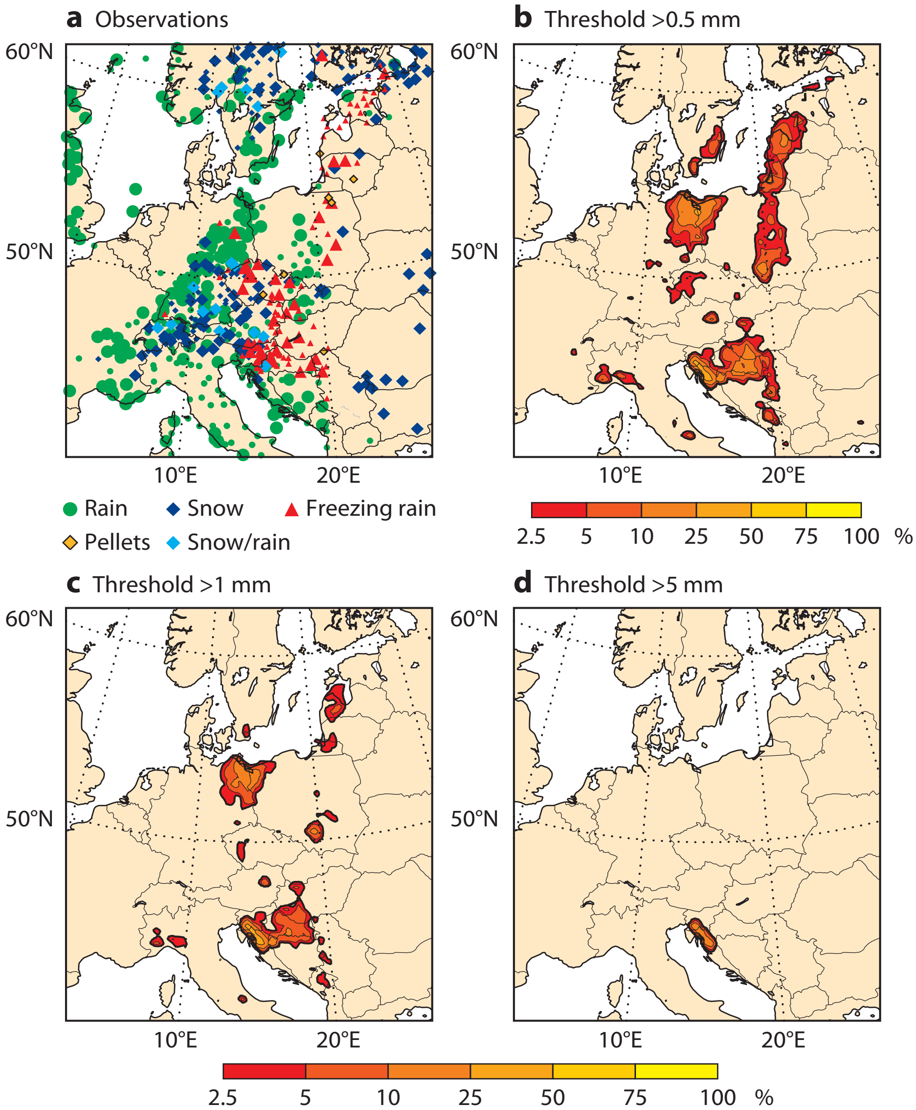

Figure 5 (a) Observations from SYNOP reports of precipitation type on 2 February 2014. Probability (%) of freezing rain accumulation greater than the specified threshold on day 3 of the forecast valid on 2 February 2014 (48-hour to 72-hour period) from the ensemble forecast (ENS) for (b) > 0.5 mm, (c) > 1 mm and (d) >5 mm. Small accumulations are widespread in general agreement with the observations apart from on the Polish/German border. The highest accumulations are indicated over part of Slovenia and Croatia, close to the region where the significant freezing rain accumulations were observed.

the north–south band of freezing rain across central Poland and the Baltic states, and a region either side of the Baltic Sea (Sweden/Germany/Poland). The highest probabilities of over 30% are present for Slovenia and Croatia. Although the Germany/Poland/Sweden Baltic Sea region was not in the observed SYNOP reports, there was a clear band of freezing precipitation further east as noted above.

Considering the 1 mm and 5 mm thresholds in Figures 5c and 5d respectively, the focus shifts to Slovenia and northern Croatia where some of the heaviest freezing rain and devastating impacts occurred. However, the accumulations and the probabilities are relatively low and this may be partly due to the resolution of the ENS. The event in Slovenia is barely resolved in the T639 (32 km) resolution ensemble, but this will improve with the ENS resolution upgrade to 20 km planned for 2015.

Case study 2: December 2013, south-eastern Canada

From 21 to 22 December 2013 a mix of snow, ice pellets and freezing rain affected the north-eastern USA and south-eastern Canada, causing significant disruption, power loss to 500,000 households, flight delays and highway accidents on one of the busiest travel weekends of the year.

Figure 6a shows the SYNOP reports of precipitation type at 06 and 12 UTC on 22 December. Similar to the European case study, the short-range HRES with new physics is able to predict a long band of freezing rain in the region where this is observed (Figure 6c), whereas the operational model used at the time predicts snow with only a few isolated spots of freezing rain along the rain/snow boundary (Figure 6b). Note also that with the new physics there is a narrow band of ice pellets predicted along the shallow leading edge of the elevated warm layer, where the snow particles

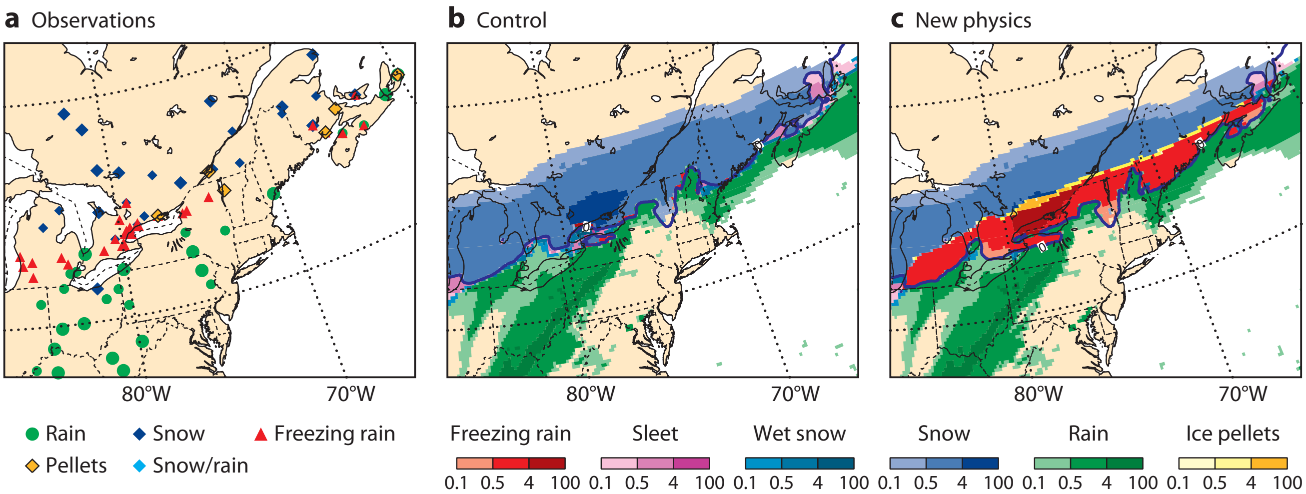

Figure 6 A significant freezing rain event over eastern North America on 22 December 2013. (a) Observations from SYNOP and METAR reports of precipitation type at 06 and 12 UTC. Precipitation rate and type from the 9-hour forecast from the 00 UTC analysis on 22 December 2013 using (b) the current operational model as the control and (c) the model with the new physics. Shading in (b) and (c) is for 0.1, 0.5 and 4 mm hr^{-1} and the thick blue contour is the 2-metre 0ºC isotherm.

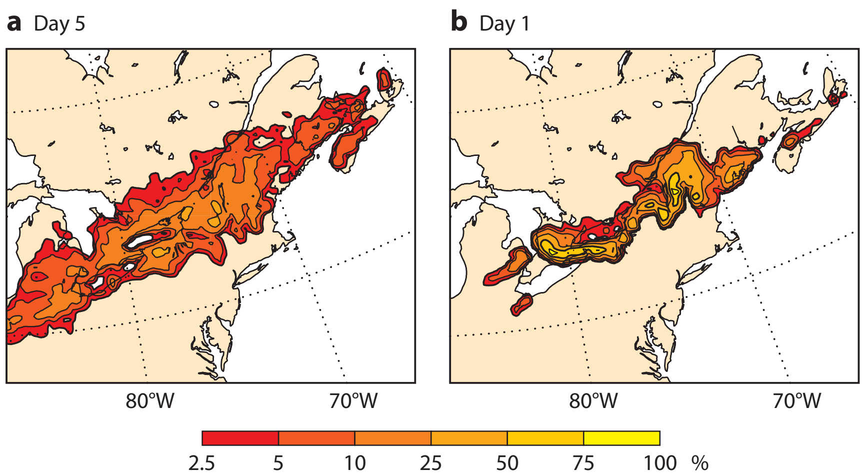

Figure 7 Probability (%) of freezing rain accumulation of more than 5 mm during the 24 hour period on 22 December 2013 from ENS for (a) five-day and (b) one-day forecast lead times, showing low probabilities for the longer lead time in the region where freezing rain was observed (Figure 6a) and probabilities increasing significantly at shorter lead times.

falling through do not completely melt and refreeze rapidly to solid particles in the cold air below. Although there are only a few SYNOP reports of ice pellets, the narrow band is unlikely to be sampled well. Case studies of other events have observed this band of ice pellets along the boundary between snow and freezing rain (*Czys et al.*, 1996).

The probability of freezing rain accumulations greater than 5 mm in the ENS with the new physics at two lead times is shown in Figure 7 for this case. At a lead time of five days, there is a band of low probability (10%–25%) of freezing rain in the right region. Probabilities increase substantially for a one-day lead time and become more focused, with values reaching more than 50% in the approximate region of the observed freezing rain, providing potentially useful information that a significant freezing rain event was expected in the area.

Outlook

Freezing rain can cause extensive disruption and damage when it is heavy and/or prolonged, and even small amounts can be very problematic, so it is an important high-impact weather phenomenon to forecast. The IFS cloud and precipitation physics is modified in IFS cycle 40r3 to represent the physics of supercooled rain and a new precipitation type diagnostic is made available to signify the presence of freezing rain in model output, as well as rain, snow, wet snow, mixed rain/snow and ice pellets. Freezing rain predictions have been evaluated for a number of case studies, two of which are shown here, to highlight the potential for the IFS to provide guidance in predicting these events.

Although the basic physics of freezing rain is present in IFS cycle 40r3, freezing drizzle associated with the coalescence of supercooled liquid water drops in relatively shallow sub-freezing boundary layer cloud is not yet represented. Future developments to the IFS will include representation of freezing drizzle production and potentially more sophisticated microphysics of the melting and freezing processes. An appropriate representation of the uncertainties in freezing rain processes is a further topic for investigation to help provide more reliable probabilities of occurrence in the ensemble.

At this stage, precipitation type with the freezing rain category is considered to be an experimental product and must be used in conjunction with the amount of precipitation to be a useful indicator of freezing rain events. Although the initial evaluation for a number of case studies shows promise, further work is required to assess the ability of the IFS to predict the probability of freezing rain at different forecast ranges – feedback about the experimental products is welcome.

FURTHER READING

Call, **D.A.**, 2010: Changes in ice storm impacts over time: 1886–2000. *Wea. Climate Soc.*, **2**, 23–35.

Carrière, **J.-M.**, **C. Lainard**, **C. Le Bot** & **F. Robart**, 2000: A climatological study of surface freezing precipitation in Europe. *Meteorol. Appl.*, **7**, 229–238.

Czys, **R.R.**, **R.W. Scott**, **K.C. Tang**, **R.W. Przybylinski** & **M.E. Sabones**, 1996: A physically based, nondimensional parameter for discriminating between locations of freezing rain and ice pellets. *Wea. Forecasting*, **11**, 591–598.

Zerr, **R.J.**, 1997: Freezing rain: An observational and theoretical study. *J. Appl. Meteorol.*, **36**, 1647–1661.

Twenty-five years of IFS/ARPEGE

JEAN PAILLEUX, JEAN-FRANÇOIS GELEYN, MATS HAMRUD, PHILIPPE COURTIER, JEAN-NOËL THÉPAUT, FLORENCE RABIER, ERIK ANDERSSON, DAVID BURRIDGE, ADRIAN SIMMONS, DEBORAH SALMOND, RYAD EL KHATIB, CLAUDE FISCHER

The coding of the first version of the IFS/ARPEGE model was initiated by Philippe Courtier and Mats Hamrud at ECMWF in 1987 as a project involving ECMWF and Météo-France – IFS: Integrated Forecasting System and ARPEGE: Action de Recherche Petites Echelles Grandes Echelles. Many scientific projects, sub-projects, and operational and research options have been built around this initial code since then, both on data assimilation and forecasting aspects.

Here, we first describe the rationale for the project, which was originally based mainly on the limitations of the optimum interpolation (OI) assimilation systems that were widely used at the time. We then describe the operational implementation of IFS/ARPEGE before going into more detail on the developments concerning variational assimilation and the spectral model. This is followed by a discussion of various scientific projects associated with IFS/ARPEGE. Finally we describe the recent evolution of IFS/ARPEGE and future developments, and look back at what has been achieved over more than 25 years of cooperation.

The scientific rationale

The main scientific trigger for the project (which was new and somewhat revolutionary in 1988) was variational data assimilation. By that time several studies had already been performed on variational assimilation, most of them theoretical. However, variational techniques were seen as a promising way to cope with several important limitations in multivariate OI assimilation systems such as those then operational at ECMWF and elsewhere.

- Inconsistency between an OI initial state and the dynamics of the forecast model, which created spurious shocks called 'spin-up effects' during the first time steps of the model integration. This led to significant loss of observational information in the form of noise.
- Difficulties in using observations reporting meteorological quantities which are linked in complex ways to temperature, humidity, pressure or winds, especially satellite observations. Consequently, with OI there was only a small impact from satellite data (radiance measurements from TOVS), in spite of rapidly increasing numbers of good quality satellite instruments.
- Challenge of producing a good analysis at the large horizontal scales, as OI by necessity was becoming more and more localized with higher observation density from new satellite instruments.

A variational assimilation comprises solving a minimization problem either at a given time in three-dimensional space (3D-Var) or over a time window preceding the model forecast (4D-Var). A 4D-Var algorithm requires the repetitive use of the forecast model over its time window, and of the adjoint of the forecast model (for computing the derivatives needed to perform the minimization efficiently). Such a 4D-Var system has to be coded around a forecast model, its tangent linear version and the latter's adjoint version – see Box A.

In 1987, at ECMWF, the need for a tangent linear and adjoint model was an important factor in the decision to code a completely new model rather than adapt the previous model code. The adjoint and tangent linear models were also seen as necessary ingredients because they are useful not only for running 4D-Var, but also for computing the forecast sensitivity to the initial state, and for computing Singular Vectors (SV) for an ensemble prediction system (these selectively sample initial perturbations with the fastest growth rate).

The development of ECMWF's forecasting system was therefore strongly based on the limitations of OI that was widely used up to that time. The introduction of variational data assimilation was built on theoretical ideas from universities in France and at Météo-France. This brought teams at ECMWF and Météo-France together into what became a collaborative effort that has been very productive now for 25 years. In fact a common global NWP system emerged called IFS by ECMWF and ARPEGE by Météo-France. To this date, new model cycles are linked having Reading or Toulouse variants.

Among the other important scientific ingredients which justified the launch of a new forecast model at Météo-France were the needs for:

- A semi-Lagrangian version of a spectral code.
- A global ARPEGE model with a variable mesh (stretching the global coordinate and tilting the pole of dilatation towards the area of maximum interest).

An important new feature of the IFS/ARPEGE was its 'integrated' property (the 'I' of 'IFS'). The idea was to have a code that is sufficiently general, flexible and modular to take an integrated approach to all the computations necessary for a global data assimilation and forecasting system: observation processing, assimilation, forecast model and post-processing feeding the data bases for forecasters (and other users). Previously, analysis, forecast model and postprocessing codes were developed independently, which often led to inconsistencies in the forecasting suite.

AFFILIATIONS

Jean Pailleux (retired), **Jean-François Geleyn**, **Ryad El Khatib**, **Claude Fischer**: Météo-France, Toulouse, France

Mats Hamrud, **Jean-Noël Thépaut**, **Florence Rabier**, **Erik Andersson**, **Deborah Salmond**: ECMWF, Reading, UK

David Burridge, **Adrian Simmons**: retired from ECMWF

Philippe Courtier: Commissariat Général au Développement Durable, Paris, France

Four-dimensional data assimilation

A

The dynamics and physics of the forecast model are an integral part of 4D-Var. Consequently 4D-Var propagates information horizontally and vertically and uses observations in a meteorologically more consistent way. The aim is to seek the initial conditions such that the forecast best fits the observations within the assimilation interval.

- 4D-Var is based on minimization of a cost function which measures the distance between the model from the observations and from the background state. The cost function and its gradient are needed for efficient minimization.
- The tangent linear model provides a computationally efficient (although approximate) way to calculate the model trajectory, and from it the cost function.
- The adjoint model is a very efficient tool to compute the gradient of the cost function.

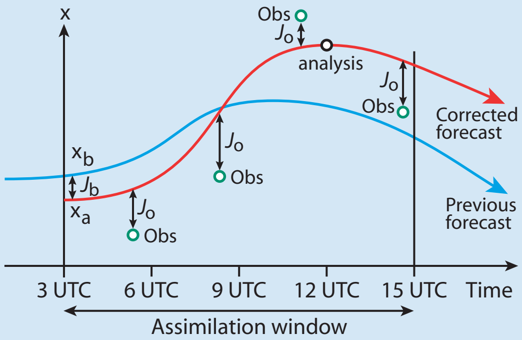

The figure shows a simplified view of the 4D-Var assimilation technique for a single parameter x. Over a given time window (12 hours here), the observations are compared at their appropriate time with a short-range forecast from the previous analysis. The model state at the initial time of the window is then adjusted to achieve a statistically good compromise between the fit J_b to the previous forecast x_b, and the fit J_o to the observations.

From the kick-off meeting of October 1988 until now, the IFS/ARPEGE system has been developed along the above-mentioned scientific lines. Also some additional projects that were not foreseen initially were initiated later on either for scientific reasons (e.g. development in France of a limited-area model called ALADIN) or for software reasons (e.g. change of computer type).

Operational implementation of IFS/ARPEGE

The first operational use of the IFS/ARPEGE code occurred in autumn 1992, both at Météo-France (replacement of the previous global spectral forecast model EMERAUDE by the ARPEGE code at the same T79 resolution, but without stretching-tilting) and at ECMWF (computation of singular vectors for the first operational implementation of the ensemble prediction system). 1993–95 was the period when major changes were made to the model component of the code.

- At Météo-France in October 1993, a stretched-tilted version of ARPEGE became operational in Eulerian mode.
- At ECMWF in March 1994, the IFS model code replaced the original operational spectral model.
- At Météo-France in October 1995, ARPEGE became semi-Lagrangian with a significant resolution increase.

From 1996 to 2000, the global analysis components were completely changed, both at ECMWF and Météo-France, from an OI to a 3D-Var system first, then from 3D-Var to 4D-Var. The operational implementation of 4D-Var occurred in November 1997 at ECMWF and in June 2000 at Météo-France. Although somewhat delayed with respect to the initial plans, they are the only two operational 4D-Var systems implemented before the end of the 20th century.

So far the 21st century has been a period of less intense development of the IFS/ARPEGE systems. However, numerous new observation types have become available, such as infrared hyperspectral sounders and GPS meteorological data. Research on these data types and then their operational implementation have shown the efficiency of variational assimilation schemes for drawing the benefits from these new observations.

The 4D-Var version has been developed to work on time windows of different length (typically of 6, 12 or 24 hours). Also the 3D-Var system has been adapted for the limited-area ALADIN model (used operationally in France and several other countries of the ALADIN consortium). IFS/ARPEGE developments also led to operational suites with increasing room given to ensemble systems and the characterisation of the uncertainty in the analysis and forecast. This is a general tendency in NWP, not limited to ECMWF and Météo-France.

Building an SI-SL spectral model with several numerical options

Since 1983, both ECMWF and Météo-France have used spectral models (with a triangular truncation) for operational NWP. Unlike the 1983 models, the design of the IFS/ARPEGE model included a semi-implicit semi-Lagrangian (SI-SL) version as the main numerical tool for high-resolution operational forecasting along with a tangent linear version and its adjoint.

The preliminary tests of 4D-Var assimilation used a barotropic model. Shortly afterwards, the baroclinic version of a primitive-equation Eulerian semi-implicit (SI) spectral model became available, together with its tangent linear and adjoint, at least for its dynamical part (almost no physical process included). This version was used for several years as the main research tool for 4D-Var and for ensemble prediction. It also paved the way for operational implementation of the ARPEGE and IFS forecasting models.

Rather than developing a single physical parametrization package for IFS/ARPEGE, dynamical–physical interfaces were set up to accommodate:

- An ARPEGE physical package, oriented towards short-range forecasting (the main job of ARPEGE).
- An IFS physical package, largely based on the physics which was operational at ECMWF at this time (in the predecessor of the IFS).

Both packages had many options, with several switches giving the flexibility to run different physical processes treated in different ways, and different techniques to link the physical and dynamical processes. The price to pay for this additional flexibility was increased complexity in the code.

At ECMWF, the operational stage for a semi-implicit, semi-Lagrangian (SI-SL) spectral model was reached in September 1991, not with the IFS code, but with its predecessor. However, March 1994 is considered as the birth of the IFS as an operational system. This mainly involved a change of code with no important changes to the science or resolution, which remained as T213L31.

At Météo-France, it appeared that combining the technical difficulties of a semi-Lagrangian scheme with the ones having a stretched geometry was leading to slightly more complexity than initially envisaged. Consequently, ARPEGE went into operations in four steps from September 1992 to October 1995. During this period ARPEGE went from a semi-implicit Eulerian formulation at T79L15/c1 to semi-Lagrangian at T149L27/c3.5 (see Box B for more details).

Evolution of the horizontal resolution in the operational forecast models IFS and ARPEGE from 1992 to 2013

B

For about 20 years, both ECMWF and Météo-France have run daily a global high-resolution forecast model, called IFS at ECMWF and ARPEGE at Météo-France. This table shows the progress made on the horizontal resolution during this period for ARPEGE and IFS. Other versions of IFS/ARPEGE have been run operationally, such as ensemble systems (ENS at ECMWF and PEARP at Météo-France). The horizontal resolution of the ensemble forecast has been generally twice as coarse as the high-resolution forecast.

The resolution is noted Txxx/Lyyy/cz, where xxx is the spectral resolution, yyy the number of levels in the vertical, z the stretching factor (always 1, no stretching, omitted for the IFS). When the model formulation started to use a linear grid, instead of a quadratic one (in 1998), the truncation is noted T_L instead of T.

September 1992	First operational version of ARPEGE forecast model which replaces the global model EMERAUDE. Same resolution, same geometry, no stretching (c=1). Semi-implicit Eulerian formulation.	T79/L15/c1
October 1993	First operational version of stretched ARPEGE forecast model (c=3.5) which replaces both the previous ARPEGE and the limited-area model PERIDOT.	T95/L21/c3.5
December 1993	The horizontal resolution of ARPEGE is increased from T95 to T119, and the vertical resolution from 21 to 24 levels.	T119/L24/c3.5
March 1994	First operational version of IFS forecast model which replaces the previous global ECMWF model. Same resolution, same geometry. semi-implicit, semi-Lagrangian formulation.	T213/L31
October 1995	ARPEGE becomes semi-Lagrangian.	T149/L27/c3.5
April 1998	IFS spectral resolution is increased by 50%. Introduction of a two-time-level semi-Lagrangian scheme; use of a linear grid (instead of quadratic).	T_L319/L31
September 1998	ARPEGE resolution upgraded.	T199/L31/c3.5
November 2000	IFS resolution upgraded.	T_L511/L60
January 2002	ARPEGE spectral resolution is increased by 50%. Introduction of a two-time-level semi-Lagrangian scheme; use of a linear grid (instead of quadratic).	T_L298/L41/c3.5
June 2003	The stretching of the ARPEGE grid is decreased from 3.5 to 2.4, while the average spectral resolution is increased to T_L358.	T_L358/L41/c2.4
February 2006	IFS resolution upgraded.	T_L799/L91
February 2008	ARPEGE resolution upgraded.	T_L538/L60/c2.4
January 2010	IFS resolution upgraded.	T_L1279/L91
April 2010	ARPEGE resolution upgraded.	T_L798L70c2.4

Further development was carried out on the IFS/ARPEGE numerical scheme to increase the spectral resolution by 50%. This was achieved with a two-time level semi-Lagrangian scheme operated on a linear gaussian grid (instead of a gaussian quadratic grid). The linear grid went into operations in April 1998 at ECMWF and in January 2002 at Météo-France. Since then the spectral resolutions have been noted 'T_L' rather than 'T' (see Box B). More recently, following the evolution already implemented in several limited-area models, a non-hydrostatic option has been developed in the IFS/ARPEGE model (see the section on ALADIN, below).

During the 25-year period, progress was made with various numerical aspects required by data assimilation. These are described in Box C.

We now consider the progress made with various scientific projects associated with IFS/ARPEGE. These concern an integrated post-processing package, dynamical core of ALADIN, ensemble prediction system, 3D-Var in ALADIN, and variational assimilation and use of new observations.

From optimal interpolation (OI) to variational assimilation

There was a general recognition that initial data (the analysis) is of critical importance for success in forecasting the medium range. However, as already explained, from about 1986 there had been growing frustration with operational OI assimilation schemes.

Initially (in 1986), the variational approach was seen as an effective means to provide a global assimilation scheme without the need for local observation selection. Also, it was noted that 4D-Var had the potential to introduce consistent use of the dynamics in assimilation. A year later it was recognised that variational methods would provide a solid foundation for the assimilation of satellite data. For example, experimentation with so-called 'physical retrievals' at the UK Met Office or 1D-Var at ECMWF had demonstrated the benefit of using model fields as first guess for the retrieval of temperature and humidity profiles from the observed radiances – this would be possible also in 3D-Var.

Early on during the development of the variational scheme, ECMWF was able to demonstrate that 4D-Var could generate well-balanced fields on the large scales, create flow-dependent, vertically sloping corrections from single-level observations, and induce wind-field information from a time-sequence of humidity-sensitive satellite radiance observations. These important results showed that the theoretical advantages of 4D-Var would be realized in practice.

All the main building blocks of 4D-Var were already in place when 3D-Var was implemented at ECMWF in 1996. Once sufficient computer power became available to run 4D-Var, intense experimentation demonstrated that all the benefits of 3D-Var were present using 4D-Var with the additional benefits of improved dynamical consistency. Figure 1 shows the impact on the 500 hPa geopotential height of going from 3D-Var to 4D-Var with everything else

Progress made with various numerical aspects required by data assimilation

C

- Development of normal mode computation and normal mode initialisation algorithm: such an initialisation process was necessary for most of the OI assimilation schemes.
- Development of Digital Filter Initialisation (DFI): this was originally developed in the ALADIN model version (becoming operational in May 1994), then adapted to the global IFS/ARPEGE model. In Météo-France it replaced the normal mode initialisation in the operational OI code in July 1996. The DFI technique has been used in 4D-Var as a weak constraint to filter out some short waves from the evolution of the model on the 4D-Var time window.
- Development of the tangent linear/adjoint of the semi-Lagrangian model: combining the semi-Lagrangian technical constraints with the tangent linear/adjoint constraints led to a complex development which could be achieved only in the mid-1990s.
- Development of simplified physical packages together with their tangent linear/adjoint counterparts: this was necessary in the incremental 4D-Var, where tangent linear and adjoint computations are performed many times with a simplified model (lower resolution, simplified physics) to run the minimization algorithm.

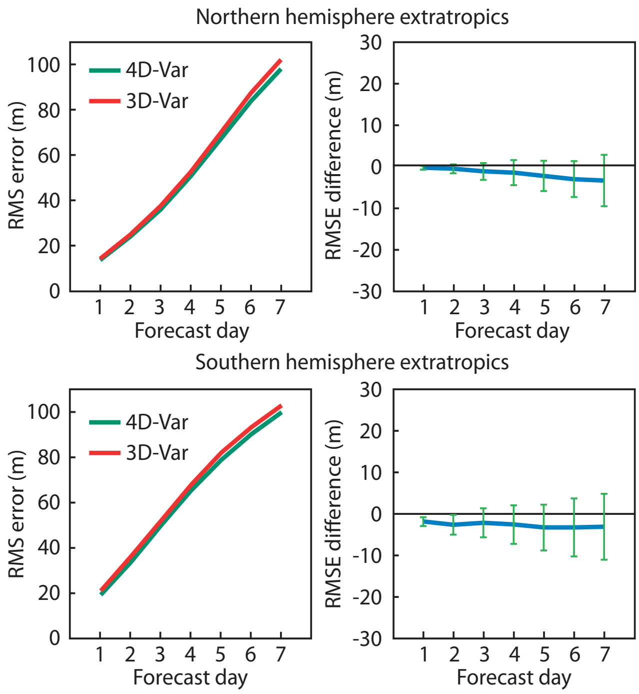

Figure 1 Comparison of root-mean-square (RMS) error for a set of pre-operational forecasts started from 3D-Var and 4D-Var analyses (left) and corresponding differences in RMS error between the two sets of forecasts with 95% confidence intervals (right) for the northern hemisphere extratropics (top) and southern hemisphere extratropics (bottom) (taken from Bouttier & Rabier, 1998, *ECMWF Newsletter No. 78*).

being kept identical. Though the impact might look small, it was an essential step towards further improvements of the assimilation system.

The development of the concept of 'incremental' 4D-Var was important for enabling an efficient first operational implementation of 4D-Var at ECMWF in 1997. At Météo-France, a few years later, the concept was expanded to keep the cost increase within a factor of 3 for its operational implementation. This led to the so-called 'multi-incremental' 4D-Var. In addition, it was necessary to introduce some filtering as part of the minimization process as well as a small degree of explicit filtering for the final result of the whole 4D-Var procedure. Last but by no means least, major effort went into developing a sophisticated linear physics package to improve the realism of the tangent-linear and adjoint models used in the 4D-Var minimization.

Dynamical core of ALADIN

An exciting possibility was offered by the development of the stretched-tilted version of ARPEGE, thanks to the novelties (with respect to IFS) of a variable map factor and of a grid-point by grid-point compass. This led to the development of a limited-area model named ALADIN. It has about 90% of its dynamical software in common with IFS/ARPEGE. Furthermore, ALADIN can share with ARPEGE the characteristics of the physics-dynamics interface as well as links with variational tools and the post-processing package known as FULL-POS (see Box D).

The basic development of ALADIN took place from 1991 to 1994 by a consortium of ten National Meteorological Services (NMSs) coordinated by Météo-France. Six other NMSs have joined the consortium since then. A key step was the signing of a software agreement between ECMWF and Météo-France. Consequently, ALADIN could benefit from most of the progress made with IFS/ARPEGE after only a small delay. But there was also a symmetric advantage: several innovations could be tested at an early stage in the ALADIN framework rather than in global conditions (e.g. parametrization schemes targeted at higher resolutions than currently used). Figure 2 shows the geographical locations of the ALADIN models that are run operationally in 2014.

FULL-POS: an integrated post-processing package

D

The post-processing package was integrated software inside the IFS, but limited to a small set of fields and only vertical interpolations on pressure levels. However, Météo-France raised the need to develop a more comprehensive post-processing package, especially to filter out the spurious waves and provide 'modern' dynamical fields such as potential vorticity or fields on isentropic levels. The forecasting model already provided the necessary tools so an extended post-processing package was developed using the same routines and numerical computations as the main model and data assimilation.

Today, FULL-POS is intensively used for its original purposes, but also for new ones. In addition, it has been regularly expanded to output new fields.

Recently, FULL-POS has been greatly modernised in the context of the OOPS project (see below the section on recent evolution) and to face the challenges of producing very high resolution forecasts on future computer architectures.

A non-hydrostatic variant, known as ALADIN-NH, was developed from 1993 to 2003; it had only minor deviations from the basic hydrostatic system used in ALADIN. This development was then brought back to the global framework and is currently being tested at ECMWF as one possible option for a new IFS configuration. ALADIN-NH has been operational at Météo-France since 2008 as the dynamical backbone of the AROME mesoscale forecasting system.

AROME and variants of the model are now being used operationally or tested by many partners within the ALADIN and HIRLAM communities.

Ensemble prediction systems

Ensemble forecasting was already being studied at ECMWF in the 1980s before the start of IFS/ARPEGE. In 1992, the first ensemble forecast was run operationally at ECMWF.

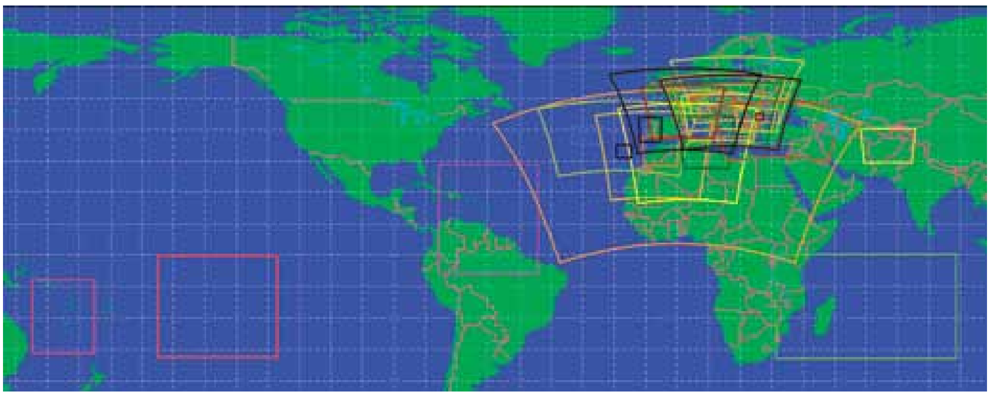

Figure 2 Map showing the domains covered by operational runs of the ALADIN model in weather services of the consortium as at spring 2014 (http://www.cnrm.meteo.fr/aladin/).

Different model runs (or members) were started from different initial states. These initial states were constructed by adding various perturbations to the standard analysis, with the perturbations intended to span the uncertainty of the initial state. The computation of these perturbations was the first operational use of the IFS/ARPEGE code at ECMWF.

Progressively, the ECMWF ensemble forecasting system improved: more members, uncertainty introduced into the forecast model, and better techniques for computing the perturbations and calibrating the ensemble scatter. In particular, the construction of initial perturbations has made increasing use of the perturbations inherent to the Ensemble of Data Assimilations (EDA). In 2014 at ECMWF, the ensemble forecast (now referred to as ENS) is run twice daily up to day 15 with 51 members (i.e. 51 IFS integrations at T_L639) and is coupled with an ocean circulation model.

At Météo-France, the development of a global ensemble prediction system started later than at ECMWF, based on stretched-tilted versions of ARPEGE, and mainly oriented towards short-range forecasting (up to day 4) for Western Europe. The ARPEGE ensemble prediction (called PEARP: Prévision d'Ensemble ARPEGE) became operational at Météo-France in 2004. Nowadays it is run twice daily up to 108 hours, with 35 members (i.e. 35 stretched ARPEGE integrations at T_L538/c2.4).

Ensemble prediction systems based on a limited-area model (LAM) have been used at several NWP centres based on the ALADIN model. In particular, the large overlap between both spectral representations (global and limited-area) allows use of the so-called 'blending technique' (merging the interpolated large scales of the global model with the smaller LAM scales) as a vehicle for developing more consistent perturbations in LAM ensembles. At Météo-France a higher resolution ensemble system has been developed based on the AROME model.

3D-Var in ALADIN and AROME

Efforts to implement a LAM configuration of the variational assimilation code of the IFS/ARPEGE software started in the years 1996–1997. However, before this time, a LAM data assimilation already effectively existed in ALADIN as a part of the OI code. A major motivation for the development of these systems was to enable the assimilation of local (national, say) observations in a regional data assimilation system in addition to any observation type already made available to the LAM via the shared IFS/ARPEGE framework. Another motivation was to complement the global assimilation system with a local one, whose corrections to a given forecast state would encompass much finer scales than those of the global system.

Some key articles about the development of IFS/ARPEGE

- Variational algorithms for analysis and assimilation of meteorological observations: theoretical aspects. 1986, *Tellus*, **38A**, 97–110.
- Application du contrôle optimal à la prévision numérique en météorologie. 1987, ***Thèse de doctorat de l'Université Pierre et Marie Curie (Paris VI)***.
- ECMWF's 4D-Var data assimilation – the genesis and ten years in operations. 2008, ***ECMWF Newsletter No. 115***, 8–12.
- A global numerical weather prediction model with variable resolution - Application to the shallow-water equations. 1988, ***Q. J. R. Meteorol. Soc.***, **114**, 1321–1346.
- A strategy for operational implementation of 4D-Var, using an incremental approach. 1994, ***Q. J. R. Meteorol. Soc.***, **120**, 1367–1388.
- Integration of the fully elastic equations cast in the hydrostatic pressure terrain-following coordinate in the framework of the ARPEGE/Aladin NWP system. 1995, ***Mon. Wea. Rev.***, **123**, 515–535.
- Improving the efficiency of a digital filtering scheme for diabatic initialization. 1997, ***Mon. Wea. Rev.***, **125**, 1976–1982.
- Ten years of research and operational activities with the IFS. 1997, ***ECMWF Newsletter No. 75***, 2–7.
- Simplified and regular physical parametrizations for incremental four-dimensional variational assilimation. 1999, ***Mon. Wea. Rev.***, **127**, 26–44.
- The ECMWF operational implementation of four-dimensional variational assimilation. Part I: Experimental results with simplified physics. 2000, ***Q. J. R. Meteorol. Soc.***, **126**, 1143–1170.
- Impact of the digital filter as a weak constraint in the pre-operational 4D-Var Assimilation System of Météo-France, 2001. ***Mon. Wea. Rev.***, **129**, 2089–2102.
- An overview of the variational assimilation in the ALADIN/France numerical weather-prediction system. 2005, ***Q. J. R. Meteorol. Soc.***, **131**, 3477–3492.
- The use of an ensemble approach to study the background error covariances in a Global NWP Model. 2006, ***Mon. Wea. Rev.***, **134**, 2466–2489.
- ECMWF's 4D-Var data assimilation – the genesis and ten years in operations. 2008, ***ECMWF Newsletter No. 115***, 8–12.
- Dynamical kernel of the Aladin-NH spectral limited-area model: revised formulation and sensitivity experiments. 2010, ***Q. J. R. Meteorol. Soc.***, **136**, 155–169.
- A new method for generating initial condition perturbations in regional ensemble prediction system: blending. 2014, ***Mon. Wea. Rev.***, **142**, 2043–2059.

As a concrete outcome, the first two 3D-Var LAM data assimilation suites became operational in 2005 in Hungary and at Météo-France. As of today, about half of the sixteen ALADIN partner NMSs run 3D-Var operationally.

At present, ALADIN 3D-Var is still operated at Météo-France for its overseas applications. An even more appealing application is the 3D-Var system becoming the backbone of the AROME data assimilation for the convection-permitting forecasting system. For example, it has been extended to assimilate ground-based radar observations and work is ongoing to implement very high frequency 3D-Var assimilation with a grid-mesh of about one kilometre. Furthermore, ensemble-based techniques for a convection-permitting LAM and software aspects remain important topics for collaboration in the coming years.

ALADIN and HIRLAM communities now join forces to further develop LAM applications in the same framework as the IFS/ARPEGE code, including the data assimilation component.

Development of variational assimilation and use of new observations

Collaboration between ECMWF and Météo-France greatly helped develop the Ensemble of Data Assimilations (EDA) for estimating the errors of the short-range forecast (background errors) used in the assimilation. This technique was first used at ECMWF for the production of climatological homogeneous covariances (and then heterogeneous correlations) of background errors.

At Météo-France there was the implementation of climatological but heterogeneous error variances based on EDA, allowing data density and storm track features to be represented. Research then progressed until it was possible to use the EDA to produce 'errors of the day', quantifying appropriately the errors as a function of the actual weather conditions (e.g. typically, errors are larger in active weather conditions than in anticyclones). The implementation of elaborate filtering methods was a key development at Météo-France, allowing daily estimation of background error variances from a small ensemble (six members when first implemented in 2008). This advantage is unmatched today by Ensemble Kalman filter systems, which require much larger ensemble sizes. Close collaboration on the EDA ensued with ECMWF, where the errors of the day were implemented in 2011. Since 2013, both centres have been using the EDA to produce flow-dependent correlations for the background error specification.

In the 1990s there was impressive progress at ECMWF in the use of satellite observations when going from using retrieved profiles to the direct use of radiances. The use of 'raw' AMSU-A data from the NOAA/ATOVS satellite started in 1999. This paved the way for steady advances throughout the 2000s when the number and variety of satellite observations increased tremendously. In particular, the hyper-spectral sounders AIRS and IASI could be used with a large impact on forecast performance. Météo-France directly benefited from these developments, and started a major activity on the use of satellite observations, once 4D-Var was implemented in 2000. Several important research activities initiated at Météo-France benefited both systems (e.g. development of the assimilation of AMSU radiances over land and the assimilation of ground-based GPS data).

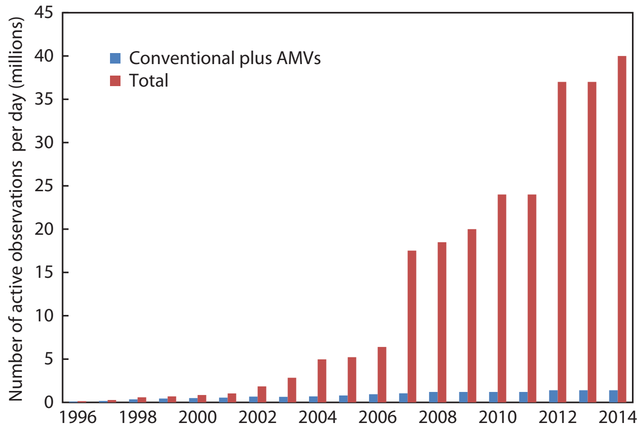

Figure 3 Evolution of the number of 'active' observations within ECMWF's 4D-Var system. Shown are the total number of observations and the number of conventional observations plus atmospheric motion vectors (AMSs). Observations are considered active if they are effectively used, indirectly used (for cloud detection, emissivity retrieval, etc.) or quality controlled and bias corrected ready to be activated (provided by Mohamed Dahoui, ECMWF).

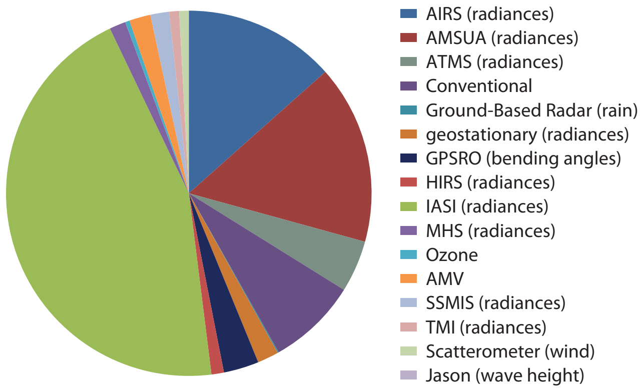

Figure 4 Contribution of observation data types to the total of 'used' data at ECMWF. The values are representative of April 2014 (provided by Mohamed Dahoui, ECMWF).

Figures 3 and 4 show the impressive increase in the amount of data assimilated at ECMWF since the implementation of 3D-Var in 1996. Similar results can be found for the ARPEGE assimilation on *http://www.meteo.fr/special/minisites/monitoring/menu.html*.

Recent evolution of the IFS/ARPEGE system and outlook

Over many years it has been necessary to face the challenge of adapting to and seizing opportunities offered by new computer architectures. A particular issue has been

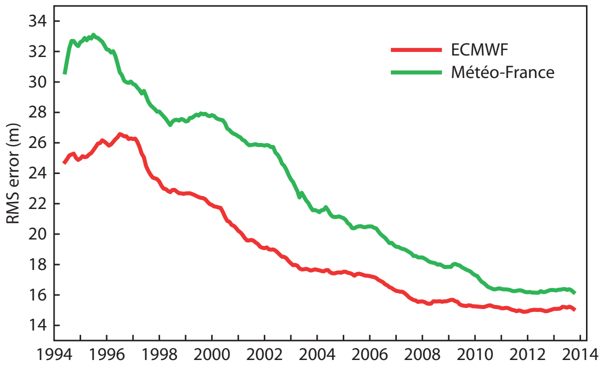

Figure 5 Root-mean-square errors for the geopotential height at 500 hPa at the 48-hour range over the northern hemisphere with respect to radiosonde observations for ECMWF (IFS) and Météo-France (ARPEGE) using a 12-month centred running mean (provided by Martin Janousek, ECMWF and Francis Pouponneau, Météo-France).

ensuring optimal code efficiency for different applications and platforms on each side of the Channel. Over the years one of the important aspects of IFS/ARPEGE has been the computer performance.

Since 1990, in terms of floating-point operations per second, the operational forecast has increased from about a Gflop to 5 Tflops running on one hundred times as many cores. Much effort has been spent on optimising and adapting the code for each new generation of computer architecture. Consequently, tight coordination for deciding on code evolution, frequency and level of code pruning, code reorganization, etc. is required. On the other hand, there is the benefit that one centre can learn from the other about strengths and weaknesses of software running on different computer systems (including the computers of the ALADIN community where the same code is run).

Radical changes to the IFS/ARPEGE system architecture have recently emerged from an initiative called OOPS (Object Oriented Prediction System). This project was initiated at ECMWF in 2010, in concert with Météo-France and the ALADIN and HIRLAM communities, based on two considerations: the IFS/ARPEGE code has increased in complexity and the current implementation of 4D-Var was considered to not be sufficiently scalable.

Object-oriented programming seemed to be a natural way to respond to the need for a more flexible, efficient and reliable code, and OOPS was initiated to address this. It is worth pointing out that although ECMWF and Météo-France are exploring different ways for evolving their global hybrid 4D-Var data assimilation systems to address the lack of scalability, OOPS will offer both organizations a common high-level flexible framework for testing alternative approaches. The OOPS development fits very well with the spirit of the long-standing collaboration between the two organizations.

More generally, improving scalability of the various components of the IFS/ARPEGE system, including a full rethinking of the dynamical core, grid mesh structures, etc., is an important challenge for NWP.

A final look back

When the IFS/ARPEGE project was initiated in the late 1980s, operational NWP was still a young scientific activity, about 20 years old in some NWP centres like Météo-France. ECMWF was about 12 years old and had been operational for less than 10 years. Forecast and analysis models used to be developed as individual pieces of software which were then assembled in an operational suite together with pre-processing and post-processing software. NWP models used to live between 5 and 10 years, sometimes less; then they were almost completely recoded either for installation on a new computer or because the code was not flexible enough to accommodate new scientific ideas. When the IFS/ARPEGE models were implemented, the EMERAUDE and PERIDOT models (predecessors of ARPEGE) had been operational for 7 to 8 years at Météo-France, and at ECMWF the predecessor of IFS had been operational for almost 11 years when replaced.

IFS/ARPEGE was designed with a different philosophy. Although the project was triggered mainly by new scientific ideas, there was a strong will to make the IFS/ARPEGE system general, flexible and modular. When the first version of IFS/ARPEGE was designed it was hoped it would live longer than its predecessors, say about 15 years.

25 years later, IFS/ARPEGE is still going strong, and both systems have shown consistently improved scores within the period (Figure 5). The current IFS/ARPEGE system is quite different from what it was 25 years ago. One could claim that some important parts of the system have been recoded several times. One could even claim that the current system should be renamed as a consequence of all these code changes, with a new name replacing 'IFS/ARPEGE'. Computer evolution has obviously had a big impact on the system. Each change of computer type required some recoding, at least to keep the operational code efficient, which could be interpreted as a lack of generality. On the other hand, to survive for more than 25 years is a good sign that the IFS/ARPEGE code has been kept sufficiently general and robust, as anticipated in its original design. Like the Phoenix of Greek mythology, it was cyclically killed and reborn.

Thinking nowadays about the scientific and technical environment when the IFS/ARPEGE project was launched more than 25 years ago, it appears very risky for at least two reasons: there was no initial guarantee that a 4D-Var assimilation was operationally feasible and many decisions had to be taken simultaneously to create a new forecast model with a stretched-tilted geometry and a new semi-Lagrangian scheme.

In addition to these two scientific challenges, the cooperative project entailed some practical considerations, such as the necessity of rapid exchange of information between tens of scientists at ECMWF and Météo-France. This aspect was helped by the explosive development of Internet and email communication which occurred at the same time.

The risks and the uncertainty were discussed intensively for several years around the launch of the project. Those who took the decision to go ahead were vindicated: a 4D-Var assimilation has now been implemented in most of the NWP centres in the world and global operational forecasts have improved considerably. But it is interesting to consider the following questions. In 1990, was there an alternative for efficient use of the new sets of satellite data? Was there an alternative for having a cost-effective high-resolution model?

Recent experiments performed at very high resolution (T7999) with fast Legendre transforms have shown that there is still a future for spectral models such as IFS/ARPEGE, in spite of the difficulties of achieving scalability with a large number of processors. The main strength of IFS/ARPEGE has been to provide a very flexible and efficient dynamical core, together with several hooks to allow the plugging of many applications, especially the more advanced data assimilation tools. Some atmospheric composition components are now also included in the system. One key feature of the system is that most of its scientific and technical developments have been a 'bottom-up endeavour' with 'top-down control' based on experience.

Improving ECMWF forecasts of sudden stratospheric warmings

MICHAIL DIAMANTAKIS

During winter a strong circumpolar cyclonic flow of cold air develops in the stratosphere which is known as the 'stratospheric polar vortex'. Observation records dating back to the 1950s show that on a number of occasions each winter this apparently stable circulation pattern can be suddenly disrupted. A warming of up to 50 K occurs in the space of just a few days (at altitudes around 30 km and above), weakening the westerly zonal-mean flow or even reversing it to be easterly in the most extreme cases. This phenomenon is called a sudden stratospheric warming (SSW) and primarily occurs in the northern hemisphere.

Figure 1 shows a time series of the mean brightness temperature at around 5 hPa in the vicinity of the north and south poles as observed by the NOAA-15 spacecraft from 1999 to the present day. This shows that in the northern polar region the seasonal variation in temperature is frequently disrupted by SSWs, but SSWs are rare in southern polar region.

It is important that our forecast model is capable of accurately predicting these dramatic events for two reasons. Firstly, despite being a stratospheric phenomenon, there is strong evidence to suggest that SSWs influence the large-scale tropospheric circulation below and therefore the winter weather that we experience. Secondly, a failure to represent the large thermal changes associated with SSWs can lead to a significant discrepancy between the model and observations (primarily from satellites). Under these conditions the data assimilation system may incorrectly interpret the mismatch as a problem with the measurements and wrongly reject perfectly good observations. Failing to use these observations (that may have helped correct the model) means that both our forecasts and analyses of these important events can be very poor.

In SSW regimes the numerical scheme currently employed by the Integrated Forecasting System (IFS) for finding the departure point of the semi-Lagrangian trajectory (SETTLS) becomes very 'noisy'. This can result in a significant under-prediction of the warming events. To address this problem a simple modification to the SETTLS will be included in the next operational cycle. The scheme identifies gridpoints that are prone to instabilities and for these a more stable scheme is applied. For the remaining points the standard SETTLS procedure is applied, which is in general more accurate when time evolution is relatively smooth.

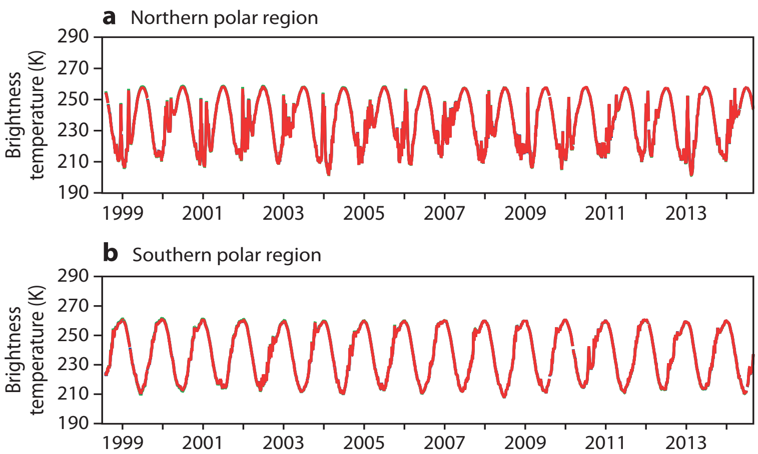

Figure 1 Time series of the mean brightness temperature observed in channel 13 of the AMSU-A instrument on board the NOAA-15 satellite. Channel 13 is sensitive to temperatures around 5 hPa. Panel (a) shows the seasonal variations in the northern polar region being disrupted by SSW events. For reference, panel (b) shows that SSWs are rare in the southern polar region.

During SSW events the new scheme shows large improvements in the accuracy of stratospheric forecasts and a significant reduction in the number of satellite observations wrongly rejected by the data assimilation system.

Different types of sudden stratospheric warming and their origin and influence

Labitzke & van Loon (1999) classify SSWs into four categories according to their strength.

- ***Major Midwinter Warmings*** occur mostly in January–February and are accompanied by a migration of the cold polar vortex south of 65°N or even a split into two separate vortices. The westerly circulation around 10 hPa is reversed to easterly and high pressure forms in the stratospheric polar region.
- ***Minor Warmings*** are strong enough to reverse the temperature gradients between the poles and mid-latitudes, but not severe enough to reverse the circulation.
- ***Canadian Warmings*** occur in early winter and may briefly change the wind direction, but they are not strong enough to cause a complete breakdown of the polar vortex.
- ***Final Warmings*** appear at the end of the winter, signalling the transition from winter to summer as the cold cyclonic stratospheric vortex is replaced by a warm high-pressure system.

Studies show that SSWs are triggered by upward propagating Rossby waves entering the stratosphere and interacting with the westerly zonal-mean flow. These vertically-propagating waves decelerate the stratospheric westerlies and their effect increases with height as the wave amplitude increases due to reduced air density. Flow disturbances grow to the point that westerlies may completely shut down and reverse to become easterlies. As this happens, air near the polar cap region descends adiabatically and intense warming occurs. For a detailed analysis the reader may consult the paper by *Matsuno* (1971).

SSWs are primarily a winter northern hemisphere phenomenon where substantial Rossby wave activity can be found. Summer conditions are not favourable for such phenomena as during the warm season strong easterlies prevail in the stratosphere and the coupling of the troposphere-stratosphere system is weak. Stratospheric warmings have a variable frequency. Almost every year will have some warming event, with a major SSW typically occurring every second year.

Are SSWs important for the weather we experience on the ground? A number of studies, for example *Baldwin & Dunkerton* (1999), have found that upper-stratospheric geopotential anomalies observed in major SSWs frequently descend into the troposphere. The process is slow and results in the typical winter westerlies being replaced in some regions by easterlies or northerlies depending on the positioning of the developing surface high-pressure system. For many parts of Europe this change is associated with cold weather. As it usually takes up to three weeks for this anomalous circulation to fully develop near the surface,

Implementation of SETTLS

A

Semi-Lagrangian (SL) schemes are used to solve numerically the transport equations of NWP. Such schemes are unconditionally stable and have good phase speed properties with little numerical dispersion. Also SL schemes have the benefit of being relatively simple – the computation of the non-linear advection term becomes part of an interpolation process in which transported fields are remapped from the fixed Eulerian model grid on the Lagrangian time-dependent 'departure point grid'.

The 'SL trajectory' equation is:

$$\frac{D\mathbf{r}}{Dt} = \mathbf{V}(\mathbf{r}, t), \quad \frac{D}{Dt} = \frac{\partial}{\partial t} + \mathbf{V} \cdot \nabla \qquad \text{(A1)}$$

where $\mathbf{D}\mathbf{r}/\mathbf{D}t$ denotes the Lagrangian derivative of the coordinates r of an air parcel which moves with velocity $\mathbf{V} = (u, v, \dot{\eta})$. The vertical wind component $\dot{\eta}$ is expressed as the time-derivative of the terrain following vertical coordinate used in the IFS. Solving the trajectory equation (A1) is an important step in every SL model as it has a big impact on forecast accuracy.

Equation (A1) is solved by discretizing its time integral in $[t, t+\Delta t]$. One discretization method often used is the second order accurate mid-point rule:

$$\mathbf{r}_\mathbf{A} - \mathbf{r}_\mathbf{D} = \Delta t\, \mathbf{V}_\mathrm{M}^{t+\frac{\Delta t}{2}}, \quad \mathbf{V}_\mathrm{M}^{t+\frac{\Delta t}{2}} \approx \mathbf{V}\left(\frac{\mathbf{r}_\mathbf{A}+\mathbf{r}_\mathbf{D}}{2}, t+\frac{\Delta t}{2}\right) \qquad \text{(A2)}$$

where M is the trajectory mid-point, D is the departure point and $\mathrm{r_D}$ its coordinates (at time t) which are unknown and must be found. The coordinates of the arrival point $\mathbf{r}_\mathrm{A}$ (defined at time $t+\Delta t$) are given and, by definition of the SL method, must be a gridpoint.

Equation (A2) defines a recurrence relation and can be solved for $\mathrm{r_D}$ using standard fixed-point iteration. At each new iteration the wind field at the trajectory midpoint is needed and is obtained using spatial interpolation. However, the wind field that needs to be interpolated is specified at future time $t+\Delta t/2$ but it has been computed only up to t. To tackle this problem in a computationally efficient manner, time extrapolation is utilised.

The IFS scheme SETTLS (Stable Two Time Level Extrapolation) is based on the formula

$$\mathbf{r}_\mathbf{A} - \mathbf{r}_\mathbf{D} = \frac{\Delta t}{2}\{\mathbf{V}_\mathrm{A}^t + [2\mathbf{V}^t - \mathbf{V}^{t-\Delta t}]_\mathrm{D}\} \qquad \text{(A3)}$$

where the term in curly brackets on the right-hand side of equation (A3) provides an approximation for the velocity at the mid-point of the trajectory and the subscript D implies interpolation of the wind field at the departure point. Once again, from equation (A3) we can define the recurrence relation

$$\mathbf{r}_\mathbf{D} = \mathbf{r}_\mathbf{A} - \frac{\Delta t}{2}\{\mathbf{V}_\mathrm{A}^t + [2\mathbf{V}^t - \mathbf{V}^{t-\Delta t}]_\mathrm{D}\} \qquad \text{(A4)}$$

which can be solved iteratively starting with $\mathbf{r}_\mathbf{D} = \mathbf{r}_\mathbf{A} - \Delta t \mathbf{V}_\mathbf{A}^t$ and cycling two further times. The final value of $\mathrm{r_D}$ becomes the departure point. In practice, the mathematical details are more complex as spherical geometry has to be taken into account.

giving an accurate medium-range prediction of a major SSW event can extend the forecast horizon of a high impact cold weather event to a timescale exceeding one month.

Semi-Lagrangian trajectories and 'numerical noise' in ECMWF model

A fundamental assumption in the semi-Lagrangian (SL) framework is that at each model instant t an air parcel starts its trajectory at a location called the 'departure point' and arrives at $t+\Delta t$ at a model gridpoint called the 'arrival point'. For each given arrival point there is a unique departure point which needs to be found. This is done by solving the so-called 'semi-Lagrangian trajectory' equation at each timestep. The solution method has been revised a few times since the introduction of the SL scheme in the IFS and the one currently used is based on scheme called SETTLS (Stable Extrapolating Two Time Level Scheme) which was developed by *Hortal* (2002). Box A describes how SETTLS has been implemented in the IFS.

SETTLS gave improved predictions compared with schemes that had been used previously. However, from an early stage it was found that noisy fields occasionally occur in forecasts in the upper part of the stratosphere, mostly when the stratospheric vortex is displaced away from the pole. As noise contaminates the vertical velocity field, large errors are introduced in the vertical transport scheme which is a key ingredient in capturing the warming accurately.

Other formulations based on extrapolation do exist. However, as demonstrated by *Hortal* (2002), SETTLS is preferable as it has better stability than the other schemes. SETTLS plays a central role in the IFS as it is also used to extrapolate nonlinear terms in the semi-implicit time integration scheme. However, in this article we will confine our discussion to the application of SETTLS in the SL trajectory equation. This particular scheme is often called SETTLST, while the corresponding scheme applied to semi-implicit computations is called SETTLS.

Despite the improvements that SETTLS and SETTLST introduced into the IFS, testing showed that very noisy fields at model levels lying in the upper half of the stratosphere sometimes occur when the night polar stratospheric jet is shifted away from the poles, a situation typical in SSWs. Experiments identified that the term which corresponds to the vertical part of vector equation used in the SETTLST (equation (A3) in Box A) is the 'numerical component' of the SL scheme that mostly contributes to noise generation.

The numerical issue does not threaten the overall stability and robustness of the model; in other words the associated instability is weak. Nevertheless, it has a negative impact on forecast error in the stratosphere. Very noisy vertical velocities result in large errors in vertical transport; this in turn affects the temperature field. Initially, the approach used for dealing with this problem was to smooth the vertical component of the wind (see *Hortal*, 2004) when the departure points were computed. However, at current resolutions smoothing has a negative impact on accuracy in the stratosphere which became apparent when it was switched off (accidentally) in IFS cycle 38r1. Because of this improvement in forecasting scores, it was decided not to re-activate the smoothing and to explore alternatives for dealing with the numerical noise problem.

Alternative techniques for smoothing have been tried and they all showed improvements in dealing with under-prediction of SSWs and noise amplification. For example, we have tested off-centring the semi-implicit scheme (a standard method to control numerical noise) and using the Iterative Centred Implicit (ICI) version of SL dynamics. However, each of these methods had its problems. Off-centring increases the damping of the numerical solver and as a result reduces the model accuracy. Gravity waves can be wiped-out if a large amount of off-centring is used. The other alternative, ICI, does not have this drawback; it is a second order accurate fully-centred scheme which in addition offers enhanced stability and for this reason it is used in the non-hydrostatic version of IFS. Improved stability comes from the fact that ICI is essentially a predictor-corrector scheme. Thus the need to extrapolate is eliminated. Unfortunately the extra benefits come at the expense of the computational cost increasing by about 30% to 40%.

As well as considering the off-centring and ICI approaches, the option of replacing the term in the vertical part of SETTLST causing the noise was investigated. The approach taken was to apply a low order non-extrapolatory scheme as described in Box B. Since this approach required only a minor change in the SL scheme and all other parts of it remained unchanged, the hope was that there would be small impact on overall model accuracy. Tests showed that this modification is successful in controlling numerical noise in the stratosphere and giving improved SSW forecasts. However, it was found that there is a clear negative impact by enforcing such change everywhere and this will be demonstrated later.

Improving the SL trajectory algorithm

It was clear that to address the problems encountered with the SETTLST there was a need for a new approach. Inspired by the findings of these experiments in which it became clear that the vertical transport and the time extrapolation in SETTLST are two crucial factors responsible for under-prediction of SSWs,

Non-extrapolatory scheme in the vertical

B

SETTLST computes the vertical component of the departure point using the formula based on equation (A4):

$$\eta_D = \eta_A - \frac{\Delta t}{2}\{\dot{\eta}_A^t + [2\dot{\eta}^t - \dot{\eta}^{t-\Delta t}]_D\}$$

Experiments indicate that it is the following extrapolation term that is causing the noise problems:

$$[2\dot{\eta}^t - \dot{\eta}^{t-\Delta t}]_D$$

This term can be replaced by $\dot{\eta}_D^t$ giving the non-extrapolatory scheme:

$$\eta_D = \eta_A - \frac{\Delta t}{2}(\dot{\eta}_A^t + \dot{\eta}_D^t).$$

a modified scheme was proposed for the vertical coordinate of the departure point. The main idea behind this modification was to identify gridpoints which have the potential to develop noise and apply the non-extrapolatory scheme described in Box B at those points while applying the standard SETTLST method elsewhere. In effect this is what we often call 'limiter' or 'filter' in NWP. The new scheme is outlined in Box C.

The modified scheme was initially tested having it active on all model levels. However, as it was found that the modified scheme improves the flow only in the stratosphere, it was finally applied only at model levels lying at or above 60 hPa. The scheme is gradually relaxed to standard SETTLS in the vertical by introducing a height dependency to the parameter β which controls the extent to which the non-extrapolatory scheme is applied; β increases gradually to 2.0 in the layer between 30 hPa and 60 hPa.

We shall call the modified scheme SETTLSTF. The letter 'F' implies that a filter is applied on the standard SETTLST; this means that the condition given in Box C is used to select those gridpoints where the non-extrapolatory scheme will be activated.

The new scheme – SETTLSTF

C

The algorithm for the vertical component of the departure point η_D is written as:

$$\eta_D = \begin{cases} \eta_A - \dfrac{\Delta t}{2}\left(\dot{\eta}_A^t + [2\dot{\eta}^t - \dot{\eta}^{t-\Delta t}]_D\right) \text{ if A} \\ \eta_A - \dfrac{\Delta t}{2}\left(\dot{\eta}_A^t + \dot{\eta}_D^t\right) \text{ if B} \end{cases}$$

$$\text{A: } \left|\dot{\eta}_A^t - \dot{\eta}_A^{t-\Delta t}\right| \le \frac{\beta}{2}\left(\left|\dot{\eta}_A^t\right| + \left|\dot{\eta}_A^{t-\Delta t}\right|\right)$$

$$\text{B: } \left|\dot{\eta}_A^t - \dot{\eta}_A^{t-\Delta t}\right| > \frac{\beta}{2}\left(\left|\dot{\eta}_A^t\right| + \left|\dot{\eta}_A^{t-\Delta t}\right|\right)$$

where $0 \le \beta/2 \le 1$.

It is a hybrid between SETTLST and the non-extrapolatory scheme given in Box B. It is applied in the vertical only, while in the horizontal the standard SETTLS is used.

The right-hand side condition in used in SETTLSTF is a simple criterion to detect gridpoints which can become noisy. This heuristic rule compares the magnitude of the vertical velocity jump during two consecutive timesteps with a two-timestep average of the vertical velocity magnitude. Big jumps are warnings that the extrapolation may produce noisy results and therefore when this occurs the non-extrapolatory scheme is activated.

The parameter β controls the extent to which the non-extrapolatory scheme is applied: for $\beta = 2$ the standard SETTLST will be applied on all gridpoints while for $\beta = 0$ the non-extrapolatory scheme will be activated everywhere. Values smaller than 2 but near to it penalise points that jump from negative to positive values as well as those that maintain the same sign but exhibit very big jumps.

Testing showed that β values near 2 are sufficient to yield satisfactory results (i.e. control noise growth and provide accurate prediction of SSW events without reducing overall accuracy of forecasts). For example, for β=1.9 about 5%–10% of the points per level switch to the non-extrapolatory scheme in forecasts at T1279L137 resolution (approximately 16 km spacing on the reduced Gaussian linear grid and 137 levels in the vertical). As expected, this percentage depends strongly on timestep which determines how much the SETTLST formula extrapolates. So for larger timesteps the non-extrapolatory scheme becomes more active.

Meteorological impact

SETTLSTF has been tested on various atmospheric flow regimes. For those having SSW events, results suggest that SETTLSTF can provide accurate predictions of stratospheric temperatures both in short and medium ranges. Noise that is usually observed in velocity and temperature fields in the stratosphere is reduced or eliminated. A consequence of these improvements is a noticeable increase in the number of satellite observations assimilated and the forecast skill in the stratosphere improves. The impact on the troposphere and on situations when no SSWs occur is neutral.

Reduction in noise with SETTLSTF

In Figures 2b & 2d the divergence field at 5 hPa is plotted for 24-hour forecasts using SETTLST and SETTLSTF. Both forecasts start from the same analysis which corresponds to the noisy divergence field shown in Figure 2a. Unlike the standard scheme, SETTLSTF produces a smooth solution. It is interesting that the gridpoints where the non-extrapolatory scheme used in SETTLSTF is triggered remain close to the noisy region as demonstrated in Figure 2c.

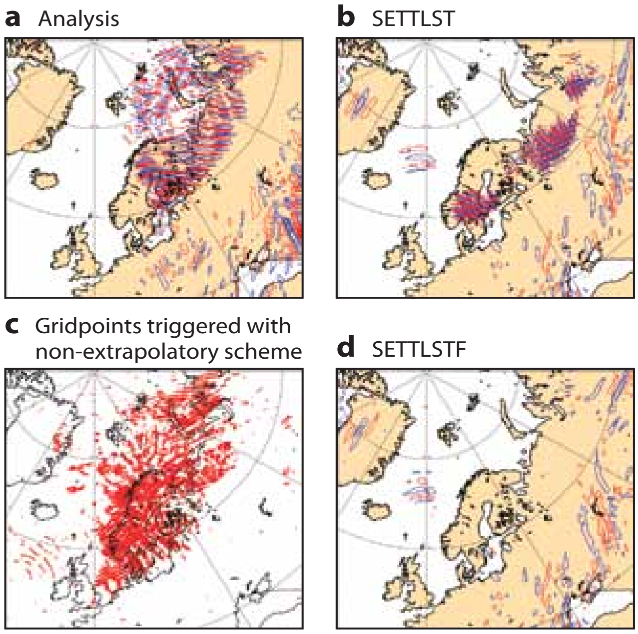

Figure 2 Divergence field at 5 hPa for (a) the analysis at 12 UTC on 15 January 2012 and 24-hour forecasts using (b) SETTLST and (d) SETTLSTF starting from the analysis given in (a). (c) Shows the gridpoints where the non-extrapolatory scheme described in Box B is triggered at 24 hours with SETTLSTF.

More importantly, the practical outcome of eliminating this noise is that SETTLSTF correctly forecasts much warmer conditions with differences exceeding 20 K even in the analysis field. This is shown clearly in Figure 3 where the 24-hour forecasts using SETTLST and SETTLSTF are compared with the corresponding analyses.

Comparing SETTLSTF with other methods

During the period from late December 2012 to mid-January 2013 two SSW events occurred. The first event took place over Siberia while the second one, a major event, was over Canada. The short-range forecast, which largely under-predicted the temperature, resulted in a frequent and large number of rejections of satellite observations. To assess the impact of the different methods for controlling the noise discussed earlier in this article, forecast experiments were run at T1279L137 resolution using the following:

- SETTLST as the control.
- SETTLST with a short timestep (Δt=2 min).
- Off-centring the semi-implicit scheme.
- Smoothing the vertical velocity.
- Iterative Centred Implicit (ICI) scheme.
- SETTLSTF.

They all start at 00 UTC on 10 January 2013 from the same analysis.

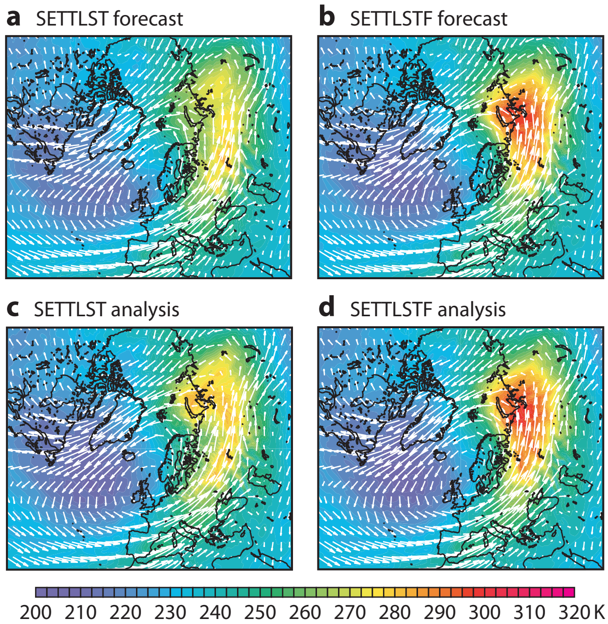

Figure 3 Temperature field at 5 hPa from two analysis (4DVAR) experiments: 24-hour forecasts from 12 UTC on 14 January 2012 using (a) SETTLST and (b) SETTLSTF. Also shown are the analyses at 12 UTC on 15 January with (c) SETTLST and (d) SETTLSTF.

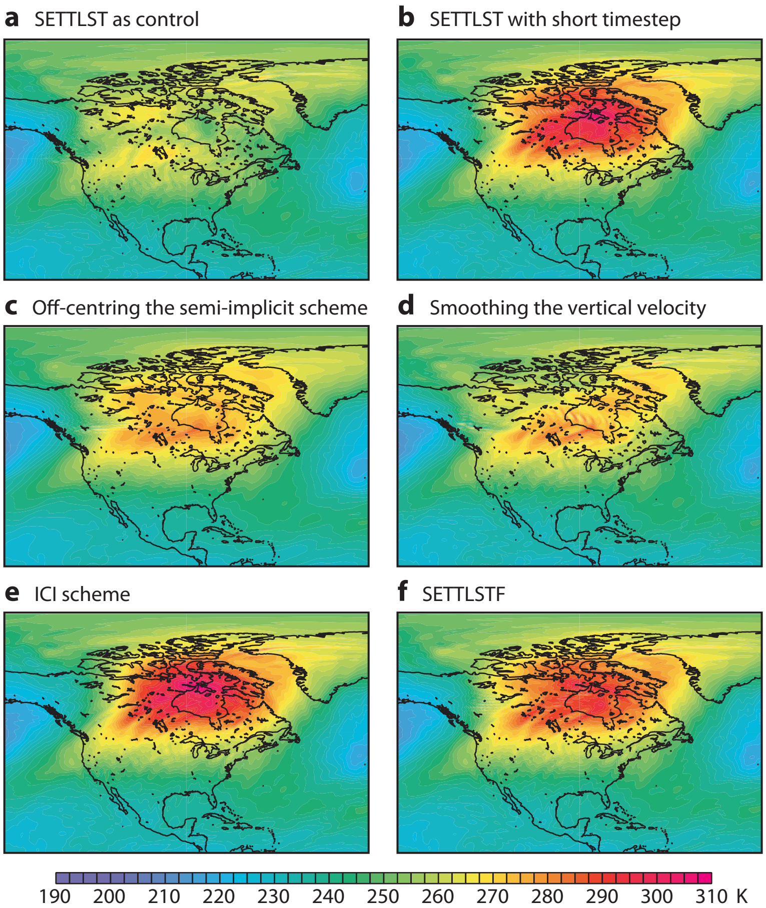

Figure 4 24-hour temperature at 5 hPa from forecasts using different SL options: (a) SETTLST as the control, (b) SETTLST with a short timestep (Δt=2 min), (c) off-centring the semi-implicit scheme, (d) smoothing the vertical velocity, (e) Iterative Centred Implicit (ICI) scheme and (f) SETTLSTF. All forecasts started at 00 UTC on 10 January 2013 from the same analysis.

The plots in Figure 4 show that the short timestep forecast (Δt=2 min) using SETTLST predicts a major warming at 5 hPa level while the standard timestep (Δt=10 min) forecast has only a very weak signal. ICI and SETTLSTF give the best results that are very close to the short timestep solution. However, SETTLSTF achieves this without increasing the computing cost. Off-centring the semi-implicit scheme improves the temperature prediction but the improvement is very moderate compared with the one obtained by ICI or SETTLSTF. The same is true for the forecast with smoothing.

Comparison against GPS radio occultation observations (not included here) confirms that the largest errors occur with SETTLST, while ICI gives the most accurate prediction closely followed by SETTLSTF. They both outperform smoothing. Furthermore, as shown in Figures 5 and 6, the new scheme can predict the warming at least one week ahead, while below model level 15 (1.2 hPa approximately) there is a very weak signal in the standard SETTLST scheme even in the one-day forecast.

Impact on the accuracy of forecasts

As mentioned earlier, using the non-extrapolatory scheme everywhere has a significant negative impact in actual forecast accuracy. This is clearly demonstrated in Figure 7a where timeseries of the Anomaly Correlation Coefficient (ACC) and Root-Mean-Square Error (RMSE) are plotted for the geopotential height field at 500 and 10 hPa for a 7-day forecast from three experiments.

- The standard SETTLST.
- The new SETTLSTF.
- The non-exploratory scheme used everywhere in the vertical.

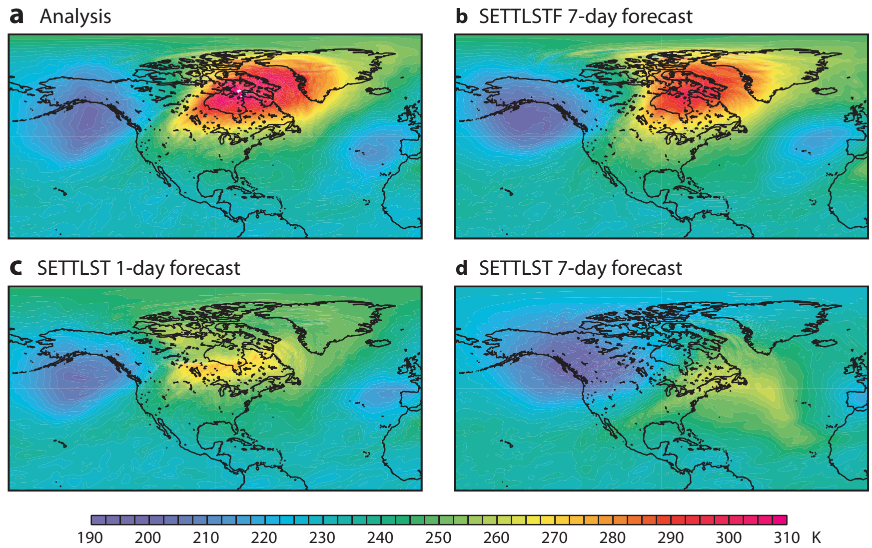

Figure 5 (a) Stratospheric temperature analysis (5 hPa) at 00 UTC on 10 January 2013 along with the corresponding 7-day forecasts using (b) SETTLSTF and (d) SETTLST. The one-day forecast using SETTLST is at (c). The plotted analysis field produced by the SETTLSTF experiment has much better agreement with observations than with SETTLST.

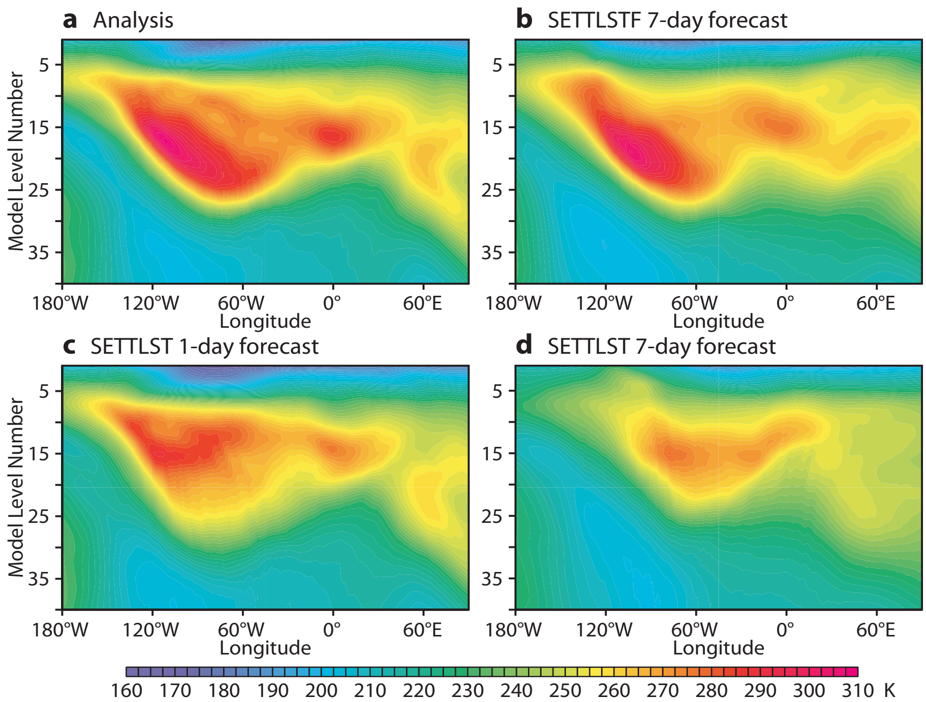

Figure 6 Vertical cross section of (a) analysed temperature at 00 UTC on 10 January 2013 along with the corresponding 7-day forecasts using (b) SETTLSTF and (d) SETTLST. The one-day forecast using SETTLST is at (c). Vertical slice corresponds to the zonal average between 50°N and 80°N.

While SETTLSTF is neutral in the troposphere, the non-extrapolatory scheme shows a consistent degradation of accuracy. In the stratosphere, as shown in Figure 7b, both SETTLSTF and the non-extrapolatory scheme perform similarly, resulting in a large reduction of RMSE (almost by a third) and an increase in ACC in the period when the SSW occurs. Further analysis of these results shows that the gains are statistically significant and justify use of this approach to satisfy the objective of improving SSW forecasting without reducing accuracy in the troposphere or in periods where such phenomena do not occur.

Additionally, there is also significant positive impact on the 4DVAR data assimilation system. Standard deviations and biases of forecast departures of brightness temperature from satellite observations in the stratosphere reduce significantly when SETTLSTF is used compared to SETTLST. These quantities are plotted in Figure 8 for various (height-dependent) channels of AMSU-A. Due to improved model predictions, satellite data rejections occurring in the assimilation cycle are also greatly reduced; for example approximately 10% more observations are assimilated at channels 11 to 14 for AMSU-A.

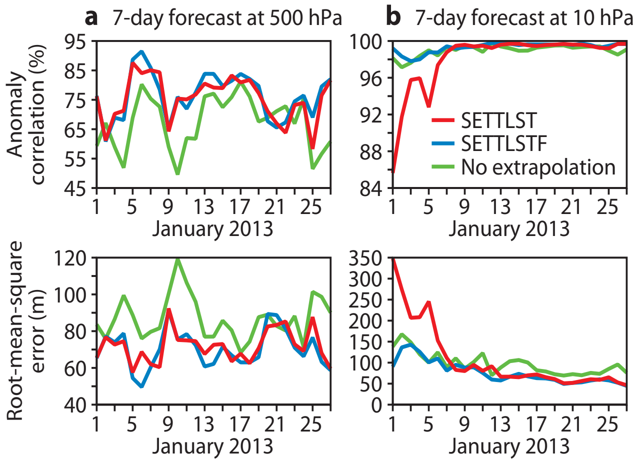

Figure 7 ACC (top) and RMSE (bottom) of the (a) 500 hPa and (b) 10 hPa geopotential for 7-day forecasts from three experiments: the standard SETTLST, new SETTLSTF and non-exploratory scheme everywhere in the vertical. Results are shown for the northern hemisphere extratropics (20°–90°N).

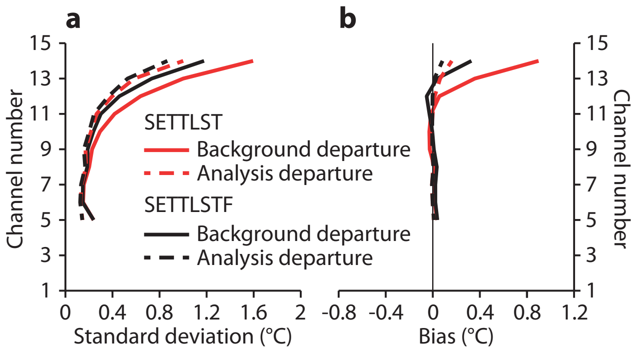

Figure 8 Standard deviation and bias of the background departure (observed minus background) and analysis departure (observed minus analysis) of brightness temperature for the northern hemisphere using SETTLSTF and SETTLST for various AMSU-A channels on board Metop-B.

Concluding remarks

A simple modification to the existing semi-Lagrangian trajectory scheme (SETTLST) is included in IFS cycle 40r3. The new scheme improves stability by identifying gridpoints which are prone to noise generation and applying there a non-extrapolating scheme that does not generate noise. It thus outperforms the standard SETTLST in numerically sensitive regions.

These modifications to the numerics improve the accuracy of forecasts, but also improve our analyses of SSWs by reducing inconsistencies between the model and satellite measurements. As a result the data assimilation system is able to exploit more observations to assist the detailed characterisation of these events.

FURTHER READING

Baldwin, M.P. & **T.J. Dunkerton**, 1999: Propagation of the Arctic Oscillation from the stratosphere to the troposphere. *J. Geophys. Res.*, **104**, 30937–30946.

Hortal, M., 2002: The development and testing of a new two-time-level semi-Lagrangian scheme (SETTLS) in the ECMWF forecast model. *Q. J. R. Meteorol. Soc.*, **128**, 1671–1687.

Hortal, M., 2004: Overview of the numerics of the ECMWF atmospheric forecast model. *ECMWF Seminar on Recent Developments in Numerical Methods for Atmospheric and Ocean Modelling*, 6 to 10 September 2004, http://old.ecmwf.int/publications/library/do/references/list/1733.

Labitzke, K.G. & **H. van Loon**, 1999: *The Stratosphere: Phenomena, History, and Relevance*. Springer Verlag, Heidelberg, 179 pp.

Matsumo, T., 1971: A dynamical model of the stratospheric sudden warming. *J. Atmos. Sci.*, **28**, 1479–1494.

ECMWF Calendar 2015

Jan 19–22	MACC-III General Assembly
Jan 26–30	Training Course: Use and Interpretation of ECMWF Products
Feb 2–6	Training Course: Use and Interpretation of ECMWF Products
Feb 11–13	Computer User Training Course: ecFlow
Feb 24–27	Computer User Training Course: GRIB
Mar 2–6	Computer User Training Course: INTRO/MARS
Mar 9–13	Computer User Training Course: Metview
Mar 16-20	NWP Training Course: Data Assimilation
Mar 23-27	EUMETSAT/ECMWF NWP SAF Training Course: Assimilation of Satellite Data
Mar 31	EUMETSAT Licensing Agents Workshop and Data Policy Group
Apr 1	Advisory Committee for Data Policy
Apr 2	ECOMET Working Group
Apr 13–17	Computer User Training Course: HPC
Apr 20–29	NWP Training Course: Predictability
Apr 21	Policy Advisory Committee
Apr 22–23	Finance Committee
May 11–21	NWP Training Course: Parametrization
May 18–22	Security and Computing Representatives' Meetings
Jun 1–5	NWP Training Course: Advanced Numerical Methods
Jun 8–10	Using ECMWF's Forecasts (UEF2015)
Jun 10–12	OpenIFS Workshop
Jun 15–19	Workshop on Advancing Training and Teaching in Numerical Weather Prediction
Jun 25–26	Council
Jun 29–Jul 3	ERA-CLIM2 Workshop on Observations for Earth System Reanalysis
Aug 31–Sep 4	Annual Seminar
Sep 28–30	Visualisation Week: Workshop on Meteorological Operational Systems
Sep 29–Oct 1	Visualisation Week: European Working Group on Operational Meteorological Workstations (EGOWS)
Oct 1 (pm)	Visualisation Week: RMetS Seminar on Visualisation in Meteorology
Oct 2 (am)	Visualisation Week: OGC MetOcean Interoperability Session
Oct 5–7	Training Course: Use and Interpretation of ECMWF Products
Oct 12–14	Scientific Advisory Committee
Oct 15–16	Technical Advisory Committee
Oct 21	Policy Advisory Committee
Oct 22–23	Finance Committee
Nov 2-6	Workshop on Extended Range Predictability
Dec 2 (pm)	Royal Meteorology Society Meeting
Dec 8-9	Council

ECMWF publications

(see http://www.ecmwf.int/en/research/publications)

Technical Memoranda

738 **Vitart**, **F.**, **G. Balsamo**, **R. Buizza**, **L. Ferranti**, **S. Keeley**, **L. Magnusson**, **F. Molteni** & **A. Weisheimer**: Sub-seasonal predictions. *October 2014*

737 **Tietsche**, **S.**, **M.A. Balmaseda**, **H. Zuo** & **K. Mogensen**: Arctic sea ice in the ECMWF MyOcean2 ocean reanalysis ORAP5. *October 2014*

734 **Chen**, **K.**, **S. English**, **N. Bormann** & **J. Zhu**: Assessment of FY-3A and FY-3B MWHS observations. *September 2014*

733 **Hamrud**, **M.**, **M. Bonavita** & **L. Isaksen**: EnKF and Hybrid Gain Ensemble Data Assimilation. *September 2014*

732 **Kazumori**, **M.**, **A.J. Geer** & **S.J. English**: Effects of all-sky assimilation of GCOM-W1/AMSR2 radiances in the ECMWF system. *October 2014*

731 **Magnusson**, **L.**, **T. Haiden** & **D. Richardson**: Verification of extreme weather events: Discrete predictands. *September 2014*

730 **Flemming**, **J.**, **V. Huijnen**, **J. Arteta**, **P. Bechtold**, **A. Beljaars**, **A.-M. Blechschmidt**, **M. Diamantakis**, **R.J. Engelen**, **A. Gaude**, **A. Inness**, **L. Jones**, **E. Katragkou**, **V.-H. Peuch**, **A. Richter**, **M.G. Schulz**, **O. Stein** & **A. Tsikerdekis**: Tropospheric chemistry in the Integrated Forecasting System of ECMWF. *September 2014*

729 **Balsamo**, **G.**, **A. Agustì-Panareda**, **C. Albergel**, **A. Beljaars**, **S. Boussetta**, **E. Dutra**, **T. Komori**, **S. Lang**, **J. Muñoz-Sabater**, **F. Pappenberger**, **P. de Rosnay**, **I. Sandu**, **N. Wedi**, **A. Weisheimer**, **F. Wetterhall** & **E. Zsoter**: Representing the Earth surfaces in the Integrated Forecasting System: Recent advances and future challenges. *October 2014*

728 **Lopez**, **P.**: Comparison of NCEP Stage IV precipitation composites with ECMWF model. *September 2014*

EUMETSAT/ECMWF Fellowship Programme Research Report

34 **Lawrence**, **H.** & **N. Bormann**: First year report: The impact of HIRS on ECMWF forecasts, adding ATMS data over land and sea ice and new observation errors for AMSU-A. *October 2014*

Index of newsletter articles

This is a selection of articles published in the *ECMWF Newsletter* series during recent years.
Articles are arranged in date order within each subject category.
Articles can be accessed on the ECMWF public website – http:// www.ecmwf.int/en/research/publications

Contact information

ECMWF, Shinfield Park, Reading, Berkshire RG2 9AX, UK

Telephone National 0118 949 9000

Telephone International +44 118 949 9000

Fax +44 118 986 9450

ECMWF's public website http://www.ecmwf.int/

E-mail: The e-mail address of an individual at the Centre is firstinitial.lastname@ecmwf.int. For double-barrelled names use a hyphen (e.g. j-n.name-name@ecmwf.int).

Problems, queries and advice	Contact
General problems, fault reporting, web access and service queries	calldesk@ecmwf.int
Advice on the usage of computing and archiving services	advisory@ecmwf.int
Queries regarding access to data	data.services@ecmwf.int
Queries regarding the installation of ECMWF software packages	software.support@ecmwf.int
Queries or feedback regarding the forecast products	forecast_user@ecmwf.int

ECMWF

Newsletter | Number 141 – Autumn 2014

European Centre for Medium-Range Weather Forecasts

www.ecmwf.int